Contemporary Mathematics
https://ojs.wiserpub.com/index.php/CM/

Research Article

Transforming Generalized Conformable Linear PDEs into Classical Linear PDEs via Generalized Conformable Integral Operators

Josué N. Gutiérrez-Corona[1], Luis A. Quezada-Téllez[2], Guillermo Fernández-Anaya[1], Jorge E. Macías-Díaz[3,4*], Ernesto Urenda-Cázares[5]

[1]Department of Physics and Mathematics, Ibero-American University, Mexico City, 01219, Mexico
[2]Apan Higher School, Autonomous University of the State of Hidalgo, Apan, Hidalgo, 43920, Mexico
[3]Department of Mathematics and Didactics of Mathematics, Tallinn University, Tallinn, 10120, Estonia
[4]Department of Mathematics and Physics, Autonomous University of Aguascalientes, Aguascalientes, 20100, Mexico
[5]Center of Exact Sciences and Engineering, University of Guadalajara, Guadalajara, 44100, Mexico
E-mail: jorge.maciasdiaz@edu.uaa.mx

Received: 12 August 2025; **Revised:** 17 October 2025; **Accepted:** 24 October 2025

Abstract: This work investigates the reduction of Generalized Conformable Partial Differential Equations (GCPDEs) to classical Partial Differential Equations (PDEs) through a tailored change of variables based on integral conformable operators. We concentrate on second-order linear PDEs due to their central role in modeling physical and engineering systems. The proposed transformation yields an equivalent equation expressed in terms of conformable derivatives, preserving the original order and degree while introducing local kernel-dependent modulation. This equivalence establishes that solving a GCPDE can be systematically reduced to solving a standard PDE in transformed coordinates. We demonstrate the utility of this framework in modeling anomalous diffusion and anisotropic transport phenomena, where traditional formulations may fail to capture essential spatial or temporal variability.

***Keywords*:** generalized conformable derivative, conformable calculus, second-order linear partial differential equations, generalized conformable integral operator, change of variables

MSC: 65L05, 34K06, 34K28

1. Introduction

The theory of conformable derivatives has emerged as a powerful framework for addressing diverse problems in applied mathematics and physics. Building on the foundational work of [1] and its generalization by [2], this paper develops a systematic approach to second-order partial differential equations using conformable calculus, with emphasis on equations involving cross-derivative terms and multivariable structures. This study focuses on second-order linear partial differential equations with two independent variables. Future research will generalize this framework to the case of n variables and nth-order linear equations, as proposed in the final conjecture of this work. Additionally, the convergence and stability of the proposed formulations under discretization, specifically focusing on numerical stability, will be analyzed in forthcoming studies.

DOI: https://doi.org/10.37256/cm.7220268236

Beyond the conformable framework, the broader field of nonlocal and generalized fractional calculus is rapidly evolving, driving the development of specialized numerical techniques for complex physical and financial domains. Recent contributions include the design of highly efficient and robust algorithms, such as the second-order accurate Alternating Direction Implicit (ADI) Galerkin technique, specifically developed to address the computational burden of three-dimensional nonlocal heat models arising in viscoelasticity [3]. Furthermore, numerical methods employing local meshless Radial Basis Functions (RBF) have shown promise for applications like numerically pricing American and European options using the time fractional Black-Scholes model in financial decision-making [4]. The rigorous investigation of generalized tempered-type integrodifferential equations, including detailed stability and convergence analyses for fully discrete schemes like 2-step Backward Differentiation Formula (BDF2) finite difference methods, also highlights the ongoing need for precise computational tools to handle generalized nonlocal operators [5]. These domain-specific advancements underscore the increasing sophistication required to model memory, non-locality, and complex scaling laws.

Recent advances in numerical methods for conformable fractional differential equations have further strengthened this field. For instance, [6] introduced a conformable non-polynomial spline method that combines finite difference and spline techniques to solve nonlinear time-fractional differential equations with unconditional stability and sixth-order convergence. Subsequently, [7] developed a logarithmic non-polynomial spline method for conformable time-fractional equations, achieving high accuracy for nonlinear inhomogeneous fractional models. These developments provide valuable computational tools that complement the analytical framework presented here.

The central contribution of this paper is the establishment of a rigorous correspondence between generalized conformable partial differential equations and their classical counterparts through a variable transformation based on conformable integral operators. This transformation preserves the order and linearity of the equations, enabling the application of classical analytical techniques within the conformable setting. The proposed framework also accommodates cross-derivative terms, extending the applicability of conformable calculus beyond previously known formulations. By linking conformable and classical Partial Differential Equations (PDEs), this approach allows the direct use of well-established mathematical results, such as existence and uniqueness theorems, maximum principles, and numerical schemes, while maintaining the flexibility to model complex diffusion and wave phenomena. The resulting methodology provides a rigorous yet computationally accessible means to study anomalous transport and heterogeneous media within a conformable context. We illustrate the effectiveness of this framework through its application to three fundamental equations: the Laplace equation, the Fokker-Planck equation, and the wave equation. These examples demonstrate its capacity to model anisotropic diffusion via spatially dependent conformable kernels, capture memory effects through temporally modulated operators, and describe dispersion in heterogeneous media. The transformation method facilitates the use of established analytical tools such as separation of variables, Fourier analysis, and similarity transformations.

The mathematical basis of our formulation stems from the Linear Extended Gâteaux Derivative (LEGD) framework [8], which generalizes differential operators. As discussed in [9–11], conformable derivatives can be regarded as specific instances of more general operator structures. Our variable transformation approach builds upon Todorov's foundational work, later adapted by [2] to the conformable context.

Second-order partial differential equations naturally arise in a wide range of scientific applications. While classical models such as the wave and heat equations are well understood, many systems involve cross-derivative terms reflecting interactions between variables or directional dependencies. Addressing these mixed derivatives requires tailored analytical tools, which the conformable framework effectively provides.

The principal contribution of this study is the development of a novel and rigorous mathematical methodology that establishes a functional equivalence between Generalized Conformable Partial Differential Equations (GCPDEs) and their classical counterparts. This is achieved via a bespoke kernel-weighted coordinate transformation, which represents a significant methodological advance by systematically accommodating second-order equations, particularly those containing complex cross-derivative terms. This transformation framework effectively unifies the analysis of complex, conformable-based models for anomalous transport with the well-established analytical power of classical PDE theory, providing a robust and versatile tool for researchers in applied mathematics and physics.

The paper is organized as follows: Section 2 presents the mathematical fundamentals and preliminaries of the conformable derivative. The rigorous requirements for mapping solutions are discussed in Section 3. Our transformation methodology is fully developed in Section 4. Section 5 demonstrates the framework's utility through detailed applications to the Laplace equation 5.1, the Fokker-Planck Equation 5.2, and the Generalized Conformable Wave Equation 5.3. The implications of our findings are discussed in Section 6, and final conclusions are drawn in Section 7.

2. Fundamentals and preliminaries of the conformable derivative

This section outlines the essential mathematical background of the conformable derivative, including its definition, properties, and distinction from the classical derivative. These foundations are key for applying the conformable approach to dynamic systems such as hydrogen turbines. The conformable derivative, inspired by the work of Khalil et al. [1], emerged as a modern tool in fractional calculus, addressing certain restrictions of traditional derivatives. It provides a flexible mathematical framework capable of describing memory and hereditary characteristics in physical and engineering contexts. Later, Gateaux expanded this concept through the extended linear Gâteaux derivative [8], introducing the generalized conformable form.

Definition 1 (Conformable function) A conformable function $h(t, \alpha)$ is differentiable in t and satisfies:

$$h(t, 1) = 1,$$

$$h(t, \alpha) \neq h(t, \beta), \quad \text{for} \quad \alpha, \beta \in (\varepsilon, 1],$$

$$h(t, \alpha) > 0, \quad \text{for all} \quad \alpha \in (\varepsilon, 1],$$

where $\varepsilon > 0$ is an arbitrarily small constant, and $\alpha \neq \beta$.

Definition 2 (Generalized Conformable Derivative) Let $h(t, \alpha)$ be a conformable function and $f : \mathbb{R} \to \mathbb{R}$ differentiable at t. The generalized conformable derivative of order α at t, denoted ${}^{h}D_t^{\alpha} f(t)$, extends integer and fractional derivatives through $h(t, \alpha)$ as

$${}^{h}D_t^{\alpha} f(t) = \lim_{\varepsilon \to 0} \frac{f(t + \varepsilon h(t, \alpha)) - f(t)}{\varepsilon}. \tag{1}$$

Here $\alpha \in (0, 1]$ regulates the scale of differentiation, enabling the operator to capture fractal and variable effects from $h(t, \alpha)$ [12]. If f is differentiable, then

$${}^{h}D_t^{\alpha} f(t) = h(t, \alpha) \frac{df(t)}{dt}. \tag{2}$$

Definition 3 (Generalized Conformable Partial Derivative) Let h be a conformable function and $f : \mathbb{R}^n \to \mathbb{R}$ differentiable at $(x_1, \ldots, x_n)$. The generalized conformable partial derivative of order α with respect to x_i, written as ${}^{h}P_{x_i}^{\alpha} f$, is given by

$${}^{h}P_{x_i}^{\alpha} f(x_1, \ldots, x_n) = \lim_{\varepsilon \to 0} \frac{f(x_1, \ldots, x_i + \varepsilon h(x_i, \alpha), \ldots, x_n) - f(x_1, \ldots, x_n)}{\varepsilon}. \tag{3}$$

For $\alpha \in (0, 1]$, this derivative represents the rate of variation of f with respect to x_i, adjusted by $h(x_i, \alpha)$. If f is differentiable, (3) simplifies to

$$ {}^{h}P^{\alpha}_{x_i} f(x_1, \ldots, x_n) = h(x_i, \alpha) \frac{\partial f}{\partial x_i}. \tag{4} $$

This formulation generalizes the classical derivative by incorporating adaptive scaling and local variability [12].

Definition 4 (Conformable Function) A function $h : \mathbb{R} \times (0, 1] \to \mathbb{R}$ is called conformable if it depends on a variable x and a fractional order α, controlling the local behavior and scale of differentiation. This function is essential in defining conformable derivatives and integrals.

Theorem 1 (Properties of the Generalized Conformable Derivative) Let $f : A \to B_1$ and $g : A \to B_2$ be α-differentiable functions with $\alpha \in (0, 1]$, for $t \in A \subset \mathbb{R}$, and $\varphi(t, \alpha) : A \times (0, 1] \to \mathbb{R}^+$. For constants $a, b, c \in \mathbb{R}$, the following hold:

1. ${}^{h}D^{\alpha}_{t} c = 0$.
2. ${}^{h}D^{\alpha}_{t}(af(t) + bg(t)) = a\,{}^{h}D^{\alpha}_{t} f(t) + b\,{}^{h}D^{\alpha}_{t} g(t)$.
3. ${}^{h}D^{\alpha}_{t}(f(t)g(t)) = f(t)\,{}^{h}D^{\alpha}_{t} g(t) + g(t)\,{}^{h}D^{\alpha}_{t} f(t)$.
4. ${}^{h}D^{\alpha}_{t}\left(\dfrac{f(t)}{g(t)}\right) = \dfrac{g(t)\,{}^{h}D^{\alpha}_{t} f(t) - f(t)\,{}^{h}D^{\alpha}_{t} g(t)}{[g(t)]^2}$.
5. ${}^{h}D^{\alpha}_{t}(f \circ g)(t) = f'(g(t))\,{}^{h}D^{\alpha}_{t} g(t)$.

Proofs of these results can be found in [12].

Definition 5 (Generalized Conformable Integral) Let $a \geq 0$, $t \geq a$, and f be defined on $(a, t]$ with a conformable function $h(t, \alpha)$ on $(a, t] \times (0, 1]$. The generalized α-order conformable integral is given by

$$ {}^{h}_{a}I^{\alpha}_{t} f(t) = \int_a^t \frac{f(\tau)}{h(\tau, \alpha)} d\tau. \tag{5} $$

The operators ${}^{h}D^{\alpha}_{t}$ and ${}^{h}_{a}I^{\alpha}_{t}$ are mutual inverses and satisfy the fundamental theorem of calculus as proven in [12].

Theorem 2 (First Fundamental Theorem for Generalized Fractional Conformable Derivatives, Theorem 10 of [12]) If f is continuous on $(a, t]$ with $a > 0$, $t > a$, and $\alpha \in (0, 1]$, then

$$ {}^{h}D^{\alpha}_{t}\left({}^{h}_{a}I^{\alpha}_{t} f(t)\right) = f(t). \tag{6} $$

Theorem 3 (Second Fundamental Theorem for Generalized Fractional Conformable Derivatives, Theorem 11 of [12]) For $a > 0$, $t > a$, and $\alpha \in (0, 1]$, if f is differentiable on $[a, \infty)$, then

$$ {}^{h}_{a}I^{\alpha}_{t}\left({}^{h}D^{\alpha}_{t} f(t)\right) = f(t) - f(a). \tag{7} $$

Remark 1 The conformable functions used in these formulations are constructed so that each parameter remains dimensionless, ensuring that physical consistency and dimensional integrity are preserved throughout the analysis.

3. Conditions for solution mapping validity

In the following, we use concepts and properties of conformable fractional derivatives without explicitly mentioning them. This is due to the fact that the theory of conformable fractional derivatives is relatively standard nowadays. However,

the reader can consult various standard references available in the literature [1, 8, 12]. To ensure the valid mapping of solutions between Generalized Conformable Partial Differential Equations (GCPDEs) and standard Partial Differential Equations (PDEs) through variable transformation, the involved functions must satisfy certain regularity conditions. The key requirements are

1. Conformable Function Regularity

• The conformable functions $h_1(x, \alpha_1)$ and $h_2(y, \alpha_2)$ must be C^2-class (continuously differentiable) in their respective domains.

• They must be non-vanishing: $h_1(x, \alpha_1) > 0$ and $h_2(y, \alpha_2) > 0$ for all x, y in the domain and $\alpha \in (0, 1]$, $x \in U$ and $y \in V$, where U, V are opensets in $\mathbb{R}$.

2. Integrability Conditions

• The integrals defining the variable transformation must be in L^1.

$$\int_a^x \frac{d\xi}{h_1(\xi, \alpha_1)} \quad \text{and} \quad \int_a^y \frac{d\tau}{h_2(\tau, \alpha_2)}$$

must be finite and well-defined over the relevant intervals.

3. Transform Invertibility

• The transformations $s(x)$ and $t(y)$ must be invertible, requiring their derivatives $\frac{ds}{dx} = \frac{1}{h_1(x, \alpha_1)}$ and $\frac{dt}{dy} = \frac{1}{h_2(y, \alpha_2)}$ to be continuous and non-zero.

4. Solution Regularity

• The solution function $f(s, t)$ must be C^2-class (twice continuously differentiable) in the domain $\Omega \subset \mathbb{R}^2$.

• The coefficients $a_{i,j}(s, t)$ and source term $g(s, t)$ must be sufficiently regular (at least C^1) to validate the transformations.

5. Dimensional Consistency

• The conformable functions $h(t, \alpha)$ must be dimensionless to preserve the physical dimensional analysis of the underlying equations.

Summary of Functional Requirements

• Function spaces: $h_1, h_2 \in C^1$ and non-vanishing; transformation integrals in L^1; $f \in C^2$ to ensure derivative existence.

• Invertibility: The variable change should define a locally smooth and invertible mapping.

These conditions guarantee that the transformation is mathematically valid and that solutions of the GCPDE properly correspond to solutions of the standard PDE under the proposed variable change.

The conditions imposed on the kernel functions, namely $h_1(x, \alpha_1) > 0$ and $h_2(y, \alpha_2) > 0$ and their required C^2-regularity, are fundamental to ensure the non-degeneracy of the transformation integrals and the smoothness of the solution mapping. Should these assumptions fail, the primary issue would be the loss of the bijective (one-to-one and onto) property, leading to either non-invertible transformations or singularities in the mapped differential equation. For instance, if a kernel function h_i vanishes within the domain, the corresponding generalized conformable derivative becomes degenerate, and the transformation integral diverges, invalidating the equivalence.

However, the methodology can be adapted to embrace operators that relax these strict conformable requirements. For cases where the kernel functions do not strictly adhere to the conformable structure (i.e., they represent a more generalized scaling than the standard conformable definition), the reduction method remains valid as long as the transformation integral remains locally C^1 and invertible. This broader class of operators falls under the umbrella of Generalized Derivative Operators (e.g., those inspired by the work of Gâteaux [8] and the extended calculus associated with Todorov's θ-derivatives [9–11]). Specifically, concepts like the Guzmán derivative [13] or Fractal derivatives [14], which define operators based on highly non-regular or fractal scaling laws, represent scenarios where the C^2 smoothness assumption fails. A closely related transformation is the Omega derivative (Ω-derivative) introduced by Castillo et al. [15], which, similar to the fractal and Guzmán derivatives, also considers different kernels to generalize the classical derivative concept.

For such systems, the method would require two potential adaptations: (i) restricting the analysis to local domains where h is well-behaved, or (ii) integrating the problem into the broader theory of extended Gâteaux derivatives, where the transformation is defined not by invertibility but by the functional properties of the resulting solution map. The core idea, that scaling operators can be eliminated via a suitable kernel-weighted coordinate change, retains its structural relevance even when the regularity assumptions are weakened.

Remark 2 In the framework of generalized conformable partial differential equations, as established in Lemma 1, the transformation between the classical partial differential equation and its conformable generalized counterpart is performed via a change of variables of the form $s = s(x)$ and $t = t(y)$. It is assumed that the mappings $s = s(x)$ and $t = t(y)$ are at least of class C^1 and admit globally defined inverses $x = x(s)$ and $y = y(t)$, which are also at least continuously differentiable.

Under these conditions, the transformation is well-defined and smooth, ensuring that the structural properties of the original differential equation are preserved under the change of variables. In particular, the generalized conformable operators act as scaled versions of the classical derivatives, modulated by the functions $h_1(x, \alpha)$ and $h_2(y, \alpha)$.

Regarding initial and boundary conditions, it follows that if the original problem involves conditions defined in terms of classical (integer-order) derivatives at specific surfaces or points (e.g., $s = s_0$ or $t = t_0$), then these must be consistently mapped to the corresponding surfaces $x = x(s_0)$ or $y = y(t_0)$ in the new variables. The conditions retain their classical nature unless an explicit conformable fractional structure is prescribed. Moreover, derivatives appearing in the conditions must be rewritten according to the chain rules derived from the transformation, involving the generalized conformable derivatives as appropriate.

Thus, provided the change of variables is well-defined, differentiable, and invertible, classical initial and boundary conditions are appropriately transferred to the conformable setting, preserving their classical (integer-order) character, unless otherwise specified.

4. Methods

In this section, we present the methodology for applying a change of variables in Partial Differential Equations (PDEs). Consider a function $f(x, y)$ defined in a domain $U \subset \mathbb{R}^2$. For clarity, we focus on the two-dimensional case. The function $f : U \to V$ is assumed to be twice continuously differentiable, i.e., $f \in C^2(U)$. We begin by considering a second-order linear PDE of the form (8).

$$a_{2,0}\frac{\partial^2 f}{\partial x^2} + a_{0,2}\frac{\partial^2 f}{\partial y^2} + a_{1,1}\frac{\partial^2 f}{\partial x \partial y} + a_{1,0}\frac{\partial f}{\partial x} + a_{0,1}\frac{\partial f}{\partial y} + a_{0,0} f = g, \tag{8}$$

where the coefficients $a_{i,j}$ are functions that depend on (x, y). We introduce the following notation for the partial derivatives:

$$f_x(x, y) = f_{1,0}, \quad f_{xx}(x, y) = f_{2,0}, \quad f_y(x, y) = f_{0,1}, \quad f_{yy}(x, y) = f_{0,2}, \quad f_{xy}(x, y) = f_{1,1}.$$

To facilitate the transformation, we propose the following change of variables presented in (9).

$$\begin{aligned} s(x) &= \int_a^x \frac{d\xi}{h_1(\xi, \alpha)}, \\ t(y) &= \int_a^y \frac{d\tau}{h_2(\tau, \alpha)}, \end{aligned} \tag{9}$$

where h_1 and h_2 are conformable functions satisfying the conditions stated in Definition 1, are sufficiently differentiable on $\mathbb{R}$, and such that the integrals defined in (9) lie in L^1. It follows (10).

$$\begin{aligned} \frac{ds}{dx} &= \frac{1}{h_1(x,\,\alpha)}, \\ \frac{dt}{dy} &= \frac{1}{h_2(y,\,\alpha)}. \end{aligned} \tag{10}$$

Assuming the inverse transformations $x = x(s)$ and $y = y(t)$ exist, we obtain the transformed partial derivatives as follows:

$$\begin{aligned} \frac{\partial f}{\partial s} &= \frac{\partial f}{\partial x}\frac{\partial x}{\partial s} = h_1 f_{1,0} = {}^{h_1}P_x^{\alpha} f, \\ \frac{\partial f}{\partial t} &= \frac{\partial f}{\partial y}\frac{\partial y}{\partial t} = h_2 f_{0,1} = {}^{h_1}P_y^{\alpha} f, \\ \frac{\partial^2 f}{\partial s^2} &= \frac{\partial (h_1 f_{1,0})}{\partial x}\frac{\partial x}{\partial s} = h_1^2 f_{2,0} + h_1' h_1 f_{1,0} = ({}^{h_1}P_x^{\alpha})^2 f, \\ \frac{\partial^2 f}{\partial t^2} &= \frac{\partial (h_2 f_{0,1})}{\partial y}\frac{\partial y}{\partial t} = h_2^2 f_{0,2} + h_2' h_2 f_{0,1} = ({}^{h_2}P_y^{\alpha})^2 f, \\ \frac{\partial^2 f}{\partial t \partial s} &= \frac{\partial (h_1 f_{1,0})}{\partial y}\frac{\partial y}{\partial t} = h_1 h_2 f_{1,1} = ({}^{h_1}P_x^{\alpha})({}^{h_2}P_y^{\alpha} f). \end{aligned} \tag{11}$$

These transformations allow the original PDE to be rewritten in terms of the new variables $(s,\, t)$, facilitating the study of conformable differential equations. It is important to highlight that if we select these changes of variables, we can rewrite the original partial derivatives as partial conformable generalized derivatives.

Remark 3 The proposed variable transformation (9) establishes a one-to-one correspondence between second-order linear partial differential equations in two variables. Consider the general second-order PDE in the (s, t) coordinate system (12).

$$a_{2,0}(s,t)\frac{\partial^2 f}{\partial s^2} + a_{0,2}(s,t)\frac{\partial^2 f}{\partial t^2} + a_{1,1}(s,t)\frac{\partial^2 f}{\partial s \partial t} + a_{1,0}(s,t)\frac{\partial f}{\partial s} + a_{0,1}(s,t)\frac{\partial f}{\partial t} + a_{0,0}(s,t) f = g(s,t), \tag{12}$$

where $a_{i,\,j} \in C^1(\Omega)$ for some open set $\Omega \subseteq \mathbb{R}^2$. Assume that the coordinate transformation given by (9),

$$x = x(s), \quad y = y(t). \tag{13}$$

We assume that this transformation is differentiable in Ω, meaning that $s(x)$ and $t(y)$ are continuously differentiable functions with nonzero derivatives. Although such a transformation may be a diffeomorphism under additional conditions, such as invertibility and the continuous differentiability of the inverse. This is not required in the present setting.

$$s'(x) \neq 0, \quad t'(y) \neq 0, \quad \forall (x, y) \in \tilde{\Omega}. \tag{14}$$

Under this transformation, the PDE is rewritten in the (x, y) coordinate system as follows:

$$A_{2,0}(x, y)\frac{\partial^2 F}{\partial x^2} + A_{0,2}(x, y)\frac{\partial^2 F}{\partial y^2} + A_{1,1}(x, y)\frac{\partial^2 F}{\partial x \partial y} + A_{1,0}(x, y)\frac{\partial F}{\partial x} + A_{0,1}(x, y)\frac{\partial F}{\partial y} + A_{0,0}(x, y)F = G(x, y), \tag{15}$$

where $F(x, y) = f(s(x), t(y))$ and the transformed coefficients $A_{i,j}(x, y)$ are given by (16).

$$\begin{aligned}
A_{0,0}(x, y) &= a_{0,0}(s(x), t(y)), \\
A_{0,1}(x, y) &= h_2(y)a_{0,1}(s(x), t(y)) + h_2'(y)a_{0,2}(s(x), t(y)), \\
A_{1,0}(x, y) &= h_1(x)a_{1,0}(s(x), t(y)) + h_1'(x)a_{2,0}(s(x), t(y)), \\
A_{1,1}(x, y) &= h_1(x)h_2(y)a_{1,1}(s(x), t(y)), \\
A_{2,0}(x, y) &= h_1^2(x)a_{2,0}(s(x), t(y)), \\
A_{0,2}(x, y) &= h_2^2(y)a_{0,2}(s(x), t(y)).
\end{aligned} \tag{16}$$

These coefficient transformations ensure that the second-order structure of the differential operator is preserved while incorporating the effects of the coordinate transformation. Furthermore, the assumptions on the smoothness and invertibility of the transformation guarantee that the resulting equation remains well-defined and retains its analytic properties in the transformed domain.

Lemma 1 Let $f : U \subset \mathbb{R}^2 \to \mathbb{R}$ be a twice continuously differentiable function, i.e., $f \in C^2(U)$, where U is an open domain. Consider the following second-order linear partial differential equation:

$$\begin{aligned}
&a_{2,0}(s, t)f_{2,0}(s, t) + a_{0,2}(s, t)f_{0,2}(s, t) + a_{1,1}(s, t)f_{1,1}(s, t) + a_{1,0}(s, t)f_{1,0}(s, t) \\
&+ a_{0,1}(s, t)f_{0,1}(s, t) + a_{0,0}(s, t)f(s, t) = g(s, t),
\end{aligned} \tag{17}$$

where the coefficients $a_{i,j} \in C^1(U)$ are continuously differentiable functions in U. Suppose we apply the change of variables proposed in (9), where the transformations $s = s(x)$ and $t = t(y)$ are at least of class C^1 and admit inverse functions $x = x(s)$ and $y = y(t)$. Then, equation (17) transforms into the following generalized conformable partial differential equation:

$$A_{2,0}(x,y)({}^{h_1}P_x^{\alpha_1})^2F(x,y)+A_{0,2}(x,y)({}^{h_2}P_y^{\alpha_2})^2F(x,y)+A_{1,1}(x,y)({}^{h_1}P_x^{\alpha_1})({}^{h_2}P_y^{\alpha_2})F(x,y)$$
$$+A_{1,0}(x,y)({}^{h_1}P_x^{\alpha_1})F(x,y)+A_{0,1}(x,y)({}^{h_2}P_y^{\alpha_2})F(x,y)+A_{0,0}(x,y)F(x,y)=G(x,y), \tag{18}$$

where $h_1 = h_1(x,\,\alpha)$ and $h_2 = h_2(y,\,\alpha)$ are conformable functions that are continuously differentiable, i.e., $h_1,\, h_2 \in C^1$. Furthermore, the functions F and G are given by the transformations $F(x,y) = f(s(x),\, t(y)$ and $G(x,y) = g(s(x),\, t(y))$.

Proof. By applying the chain rule, the partial derivatives can be expressed as shown in (11). Thus, equation (17) can be rewritten as is presented in (19).

$$A_{2,0}(x,y)({}^{h_1}P_x^{\alpha_1})^2f(s(x),t(y))+A_{0,2}(x,y)({}^{h_2}P_y^{\alpha_2})^2f(s(x),t(y))$$
$$+A_{1,1}(x,y)({}^{h_1}P_x^{\alpha_1})({}^{h_2}P_y^{\alpha_2})f(s(x),t(y))+A_{1,0}(x,y)({}^{h_1}P_x^{\alpha_1})f(s(x),t(y)) \tag{19}$$
$$+A_{0,1}(x,y)({}^{h_2}P_y^{\alpha_2})f(s(x),t(y))+A_{0,0}(x,y)f(s(x),t(y))=g(s(x),t(y)),$$

where the coefficients $A_{i,\,j}(x,\,y)$ are defined by expression (16).

Since the functions $s(x)$ and $t(y)$ are assumed to be continuously differentiable and invertible, we define $F(x,\,y) = f(s(x),\, t(y))$ and $G(x,\,y) = g(s(x),\, t(y))$. Substituting these expressions into the equation above yields.

$$A_{2,0}(x,y)({}^{h_1}P_x^{\alpha_1})^2F(x,y)+A_{0,2}(x,y)({}^{h_2}P_y^{\alpha_2})^2F(x,y)+A_{1,1}(x,y)({}^{h_1}P_x^{\alpha_1})({}^{h_2}P_y^{\alpha_2})F(x,y) \tag{20}$$
$$+A_{1,0}(x,y)({}^{h_1}P_x^{\alpha_1})F(x,y)+A_{0,1}(x,y)({}^{h_2}P_y^{\alpha_2})F(x,y)+A_{0,0}(x,y)F(x,y)=G(x,y). \tag{21}$$

This completes the proof. □

Lemma 1 establishes a correspondence between the generalized conformable partial differential equation and a second-order linear partial differential equation. Accordingly, one may assume that the variable transformation preserves the solutions. The subsequent theorem provides a formal proof of this fact.

Theorem 4 Let $f(s,\,t)$ be a function of class C^2 in a domain $\Omega \subset \mathbb{R}^2$, and let $a_{i,\,j}(s,\,t)$ and $g(s,\,t)$ be sufficiently smooth functions in Ω. Suppose that $s(x)$ and $t(y)$ are continuously differentiable and invertible transformations given by (9). If $f(s,\,t)$ is a solution of the second-order linear partial differential equation (22).

$$b_{2,0}(s,t)f_{2,0}(s,t)+b_{0,2}(s,t)f_{0,2}(s,t)+b_{1,1}(s,t)f_{1,1}(s,t)$$
$$+b_{1,0}(s,t)f_{1,0}(s,t)+b_{0,1}(s,t)f_{0,1}(s,t)+b_{0,0}(s,t)f(s,t)=g(s,t), \tag{22}$$

then the transformed function $F(x,\,y) = f(s(x),\,t(y))$ satisfies the corresponding generalized conformable partial differential equation (23).

$$B_{2,0}(x,y)({}^{h_1}P_x^{\alpha_1})^2F(x,y)+B_{0,2}(x,y)({}^{h_2}P_y^{\alpha_2})^2F(x,y)+B_{1,1}(x,y)({}^{h_1}P_x^{\alpha_1})({}^{h_2}P_y^{\alpha_2})F(x,y)$$
$$+B_{1,0}(x,y)({}^{h_1}P_x^{\alpha_1})F(x,y)+B_{0,1}(x,y)({}^{h_2}P_y^{\alpha_2})F(x,y)+B_{0,0}(x,y)F(x,y)=G(x,y), \tag{23}$$

where the coefficient functions $A_{i,j}(x,y)$ are given by (16), and the transformations $s(x)$ and $t(y)$ are defined by (9).

Proof. To prove the theorem, we substitute $F(x,y)=f(s(x),t(y))$ into equation (23) and verify that it satisfies the equation. First, we compute the partial derivatives as shown in (24).

$$({}^{h_1}P_x^{\alpha_1})F(x,y)=\left(h_1\frac{\partial}{\partial x}\right)f(s(x),t(y))=h_1f_{1,0}(s(x),t(y))s'(x)=f_{1,0}(s(x),t(y)),$$

$$({}^{h_2}P_y^{\alpha_2})F(x,y)=\left(h_2\frac{\partial}{\partial y}\right)f(s(x),t(y))=h_2f_{0,1}(s(x),t(y))t'(y)=f_{0,1}(s(x),t(y)),$$

$$\begin{aligned}({}^{h_1}P_x^{\alpha_1})^2F(x,y)&=\left(h_1\frac{\partial}{\partial x}\right)^2f(s(x),t(y))=\left(h_1\frac{\partial}{\partial x}\right)f_{1,0}(s(x),t(y))\\&=h_1f_{2,0}(s(x),t(y))s'(x)=f_{2,0}(s(x),t(y)),\end{aligned} \tag{24}$$

$$\begin{aligned}({}^{h_2}P_y^{\alpha_2})^2F(x,y)&=\left(h_2\frac{\partial}{\partial y}\right)^2f(s(x),t(y))=\left(h_2\frac{\partial}{\partial y}\right)f_{0,1}(s(x),t(y))\\&=h_2f_{0,2}(s(x),t(y))t'(y)=f_{0,2}(s(x),t(y)).\end{aligned}$$

Substituting these conformable derivatives into equation (23), we obtain (25).

$$A_{2,0}(x,y)f_{2,0}(s(x),t(y))+A_{0,2}(x,y)f_{0,2}(s(x),t(y))$$
$$+A_{1,1}(x,y)f_{1,1}(s(x),t(y))+A_{1,0}(x,y)f_{1,0}(s(x),t(y)) \tag{25}$$
$$+A_{0,1}(x,y)f_{0,1}(s(x),t(y))+A_{0,0}(x,y)f(s(x),t(y))=g(s(x),t(y)),$$

which is an identity, since the coefficients satisfy the transformation $A_{i,j}(x,y)=a_{i,j}(s(x),t(y))$. Thus, we obtain the equivalent equation presented in (26).

$$b_{2,0}(s(x),t(y))f_{2,0}(s(x),t(y))+b_{0,2}(s(x),t(y))f_{0,2}(s(x),t(y))$$
$$+b_{1,1}(s(x),t(y))f_{1,1}(s(x),t(y))+b_{1,0}(s(x),t(y))f_{1,0}(s(x),t(y))$$

$$+b_{0,1}(s(x),t(y))f_{0,1}(s(x),t(y))+b_{0,0}(s(x),t(y))f(s(x),t(y))=g(s(x),t(y)). \tag{26}$$

Since the coefficient transformation satisfies $b_{i,j}(s(x),\,t(y))=B_{i,j}(x,\,y)$, equation (26) holds as an equivalence, thereby completing the proof. □

Theorem 4 establishes a fundamental connection between second-order linear partial differential equations and their transformed counterparts under a coordinate change. This result ensures that if a function $f(s,t)$ is a solution to the original equation in the (s,t) coordinate system, then its transformed counterpart $F(x,y)=f(s(x),t(y))$ remains a solution in the new (x,y) system. The validity of this transformation relies on the smoothness and invertibility of the change of variables, which guarantees the preservation of differentiability properties. Furthermore, the theorem highlights how the structure of the differential operator is preserved under the transformation, ensuring that the solution space is mapped consistently between coordinate systems. This result is particularly useful in applications where a coordinate change simplifies the PDE, making it more tractable for analysis or numerical methods.

Rersults analogous to the Lemma 1 and Theorem 4 can be written the case of ordinary differential equations. These results are shown as follows.

Lemma 2 Let $f: I\subset\mathbb{R}\to\mathbb{R}$ be a twice continuously differentiable function, i.e., $f\in C^2(I)$, where I is an open interval. Consider the following second-order linear ordinary differential equation:

$$a_2(t)f''(t)+a_1(t)f'(t)+a_0(t)f(t)=g(t), \tag{27}$$

where the coefficients $a_0,a_1,a_2\in C^1(I)$ are continuously differentiable functions on I, and $a_2(t)\neq 0$ for all $t\in I$. Suppose we apply a change of variable $t=t(x)$, where the transformation $t(x)$ is at least of class C^1 and admits an inverse function $x=x(t)$ defined by (28).

$$t(x)=\int_a^x \frac{d\eta}{h(\eta,\,\alpha)}, \tag{28}$$

where $h=h(x,\,\alpha)$ is a conformable function that is continuously differentiable, i.e., $h\in C^1$, and $0<\alpha\leq 1$. Furthermore, the functions F and G are given by the transformations $F(x)=f(t(x))$ and $G(x)=g(t(x))$ and (28) is in L^1. Then, equation (27) transforms into the following generalized conformable ordinary differential equation:

$$A_2(x)({}^hD_x^\alpha)^2F(x)+A_1(x)({}^hD_x^\alpha)F(x)+A_0(x)F(x)=G(x). \tag{29}$$

Proof. We begin by applying the change of variable $F(x):=f(t(x))$, where

$$t(x)=\int_a^x \frac{d\eta}{h(\eta,\,\alpha)}. \tag{30}$$

Since $h\in C^1$ and $h(x,\,\alpha)>0$, the transformation $t(x)$ and transformation admits inverse $x(t)$. From (30), we have

$$\frac{dt}{dx}=\frac{1}{h(x,\,\alpha)}\quad\Rightarrow\quad\frac{dx}{dt}=h(x,\,\alpha). \tag{31}$$

Differentiating $F(x) = f(t(x))$, we obtain

$$\frac{dF}{dx} = \frac{df}{dt} \cdot \frac{dt}{dx} = f'(t(x)) \cdot \frac{1}{h(x, \alpha)}, \tag{32}$$

so that

$$f'(t(x)) = \frac{\partial f(t(x))}{\partial t} = h(x, \alpha) \cdot F'(x) = {}^{h}D_{x}^{\alpha} F(x), \tag{33}$$

throughout this work, we employ the notation $f'(t(x)) \equiv \dfrac{\partial f(t(x))}{\partial t}$ to denote the first-order partial derivative of f with respect to the variable t, where t is defined as a function of x.

For the second derivative, applying the chain rule

$$\frac{d^2F}{dx^2} = \frac{d}{dx}\left(f'(t(x)) \cdot \frac{1}{h(x, \alpha)} \right). \tag{34}$$

Using the product rule

$$\frac{d^2F}{dx^2} = f''(t(x)) \cdot \left(\frac{dt}{dx}\right) \frac{1}{h(x, \alpha)} + f'(t(x)) \cdot \frac{d}{dx}\left(\frac{1}{h(x, \alpha)}\right), \tag{35}$$

$$\frac{d^2F}{dx^2} = f''(t(x)) \cdot \frac{1}{h(x, \alpha)^2} - f'(t(x)) \cdot \frac{h_x(x, \alpha)}{h(x, \alpha)^2}, \tag{36}$$

where $h_x(x, \alpha) := \dfrac{\partial h(x, \alpha)}{\partial x}$. Solving for $f''(t(x))$, we obtain

$$\frac{\partial^2 f(t((x))}{\partial t^2} = f''(t(x))h(x, \alpha)^2 F''(x) + h(x, \alpha)h_x(x, \alpha)F'(x) = ({}^{h}D_{x}^{\alpha})^2 F(x), \tag{37}$$

throughout this section, we employ the notation $f''(t(x)) \equiv \dfrac{\partial^2 f(t(x))}{\partial t^2}$ to denote the second-order partial derivative of f with respect to the variable t, where t is defined as a function of x.

Substituting into equation (27)

$$a_2(t(x))f''(t(x)) + a_1(t(x))f'(t(x)) + a_0(t(x))f(t(x)) = g(t(x)), \tag{38}$$

$$a_2(t(x))\left[h(x, \alpha)^2 F''(x) + h(x, \alpha)h_x(x, \alpha)F'(x)\right] + a_1(t(x))h(x, \alpha)F'(x) + a_0(t(x))F(x) = G(x). \tag{39}$$

Define the new coefficients

$$A_2(x) := a_2(t(x))h(x,\alpha)^2, \tag{40}$$

$$A_1(x) := a_2(t(x))h(x,\alpha)h_x(x,\alpha) + a_1(t(x))h(x,\alpha), \tag{41}$$

$$A_0(x) := a_0(t(x)). \tag{42}$$

Then the transformed equation becomes

$$A_2(x)F''(x) + A_1(x)F'(x) + A_0(x)F(x) = G(x), \tag{43}$$

which in terms of the conformable derivative operator ${}^hD_x^\alpha$ reads

$$A_2(x)({}^hD_x^\alpha)^2F(x) + A_1(x)({}^hD_x^\alpha)F(x) + A_0(x)F(x) = G(x). \tag{44}$$

This concludes the proof. □

Theorem 5 Let $f(t)$ be a function of class C^2 in a domain $\Omega \subset \mathbb{R}$, and let $a_{i,j}(t)$ and $g(t)$ be sufficiently smooth functions in Ω. Suppose that $t(x)$ is a continuously differentiable and invertible transformation given by $t = t(x)$. If $f(t)$ is a solution of the second-order linear ordinary differential equation

$$b_2(t)f''(t) + b_1(t)f'(t) + b_0(t)f(t) = g(t), \tag{45}$$

then the transformed function $F(x) = f(t(x))$ satisfies the corresponding generalized conformable ordinary differential equation

$$B_2(x)({}^hP_x^\alpha)^2F(x) + B_1(x)({}^hP_x^\alpha)F(x) + B_0(x)F(x) = G(x), \tag{46}$$

where the coefficient functions $B_0(x)$, $B_1(x)$, and $B_2(x)$ are determined by the transformation, and $t(x)$ is defined by the inverse relationship.

Proof. To prove the theorem, we substitute $F(x) = f(t(x))$ into equation (46) and verify that it satisfies the equation. First, we compute the conformable derivatives

$$({}^hD_x^\alpha)F(x) = \left(h\frac{d}{dx}\right)f(t(x)) = hf'(t(x))t'(x) = f'(t(x)), \tag{47}$$

$$({}^hD_x^\alpha)^2F(x) = \left(h\frac{d}{dx}\right)^2 f(t(x)) = hf''(t(x))t'(x) = f''(t(x)). \tag{48}$$

Substituting these conformable derivatives into equation (46), we obtain

$$B_2(x)f''(t(x)) + B_1(x)f'(t(x)) + B_0(x)f(t(x)) = G(x), \tag{49}$$

which is an identity, as the coefficients satisfy the transformation $B_i(x) = b_i(t(x))$. Thus, we obtain the equivalent equation

$$b_2(t(x))f''(t(x)) + b_1(t(x))f'(t(x)) + b_0(t(x))f(t(x)) = g(t(x)), \tag{50}$$

thereby completing the proof. □

5. Applications

This section demonstrates the practical implementation and utility of the theoretical framework developed in Sections 3 and 4 through its application to three fundamental classes of partial differential equations. The transformation methodology established previously provides a systematic approach for analyzing and solving generalized conformable partial differential equations across diverse scientific domains. We specifically examine the Laplace equation, the Fokker-Planck equation, and the wave equation, illustrating how our framework enables the reduction of conformable PDEs to their classical counterparts through carefully constructed variable transformations. Each application includes numerical implementations that validate the theoretical results and demonstrate how varying conformable orders and kernel functions can effectively model complex physical behaviors, including anisotropic diffusion, anomalous transport phenomena, and modified wave propagation characteristics.

The choice of the kernel functions is crucial as it allows the expression of a wide range of anomalous or local memory behaviors. For the simulations presented in this section, the chosen kernel functions were restricted to those having a conformable structure to maintain consistency with the primary theoretical results. However, it is essential to note that these functions can be selected heuristically to model specific phenomenologies, or determined through a fitting process based on experimental data. In other works, such as those by [16, 17], these generalized functions have been interpreted as representing anomalous thermal or temporal delays. These case studies collectively highlight the versatility and robustness of our methodology in addressing physical systems where traditional integer-order models prove inadequate.

5.1 *Laplace equation*

The Laplace equation serves as a cornerstone for modeling steady-state phenomena in potential theory, electrostatics, and fluid dynamics. While traditional approaches rely on integer-order calculus and recent fractional methods [18] employ non-local operators with Laplace transforms, our work presents an alternative pathway through generalized conformable calculus. Unlike fractional approaches that require solution estimates of exponential order for Laplace transform applicability, our conformable formulation maintains local differentiability while capturing anisotropic behavior through dimension-specific kernel functions. This framework proves particularly advantageous for boundary value problems in rectangular domains, where the conformable operators naturally adapt to the geometry through coordinate-aligned kernel functions, offering both mathematical tractability and physical interpretability of the resulting solutions.

We consider the generalized Laplace equation in a rectangular domain with boundary conditions given on all four sides. The governing equation includes generalized fractional differential operators and variable coefficients. Our goal is to solve the problem using the method of separation of variables and to classify the solution based on the sign of the separation constant.

We consider the generalized Laplace equation of the form

$$
\begin{aligned}
&{}^{h_1}P_x^{\alpha_1} f(x,y) + {}^{h_2}P_y^{\alpha_2} f(x,y) = 0,\\
&\left(h_1(x,\alpha_1)\frac{\partial}{\partial x}\right)^2 f(x,y) + \left(h_2(y,\alpha_2)\frac{\partial}{\partial y}\right)^2 f(x,y) = 0,\\
&(h_1(x))^2\frac{\partial^2 f}{\partial x^2} + h_1(x)h_1'(x)\frac{\partial f}{\partial x} + (h_2(y))^2\frac{\partial^2 f}{\partial y^2} + h_2(y)h_2'(y)\frac{\partial f}{\partial y} = 0,
\end{aligned}
\tag{51}
$$

subject to the boundary conditions

$$
f(0,y) = 0, \quad f(p,y) = a, \quad 0 < y < q, \tag{52}
$$

$$
f(x,0) = 0, \quad f(x,q) = g(x), \quad 0 < x < p. \tag{53}
$$

In the context of the generalized Laplace equation (51), α_1 and α_2 represent the fractional orders of the conformable derivatives in the x- and y-directions, respectively, with $\alpha_1,\ \alpha_2 \in (\varepsilon,\ 1]$, where ε is a small positive number to maintain strict positivity of the orders. The functions $h_1(x,\alpha_1)$ and $h_2(y,\alpha_2)$ are the corresponding strictly positive and continuously differentiable kernel functions, which locally modulate the spatial scaling of the differential operators ${}^{h_1}P_x^{\alpha_1}$ and ${}^{h_2}P_y^{\alpha_2}$. Finally, $f(x,y)$ denotes the unknown scalar field (the solution) of the equation.

We define the following change of variables:

$$
s(x) = \int_0^x \frac{d\xi}{h_1(\xi)}, \qquad t(y) = \int_0^y \frac{d\tau}{h_2(\tau)}, \tag{54}
$$

and so the domain transforms to

$$
s(0) = 0, \quad s(p) = L, \quad t(0) = 0, \quad t(q) = H. \tag{55}
$$

In the new variables s and t, the PDE becomes the classical Laplace equation

$$
\frac{\partial^2 f}{\partial s^2} + \frac{\partial^2 f}{\partial t^2} = 0, \tag{56}
$$

with the boundary conditions:

$$
f(0,t) = 0, \quad f(L,t) = a, \quad 0 < t < H, \tag{57}
$$

$$
f(s,0) = 0, \quad f(s,H) = g(s), \quad 0 < s < L. \tag{58}
$$

Solution via separation of variables. We seek a solution in the form

$$f(s,t) = f_p(s) + \sum_{n=1}^{\infty} C_n \sin\left(\frac{n\pi s}{L}\right) \sinh\left(\frac{n\pi t}{L}\right), \tag{59}$$

where $f_p(s)$ is a particular solution satisfying the nonhomogeneous condition $f(L,t) = a$. We choose

$$f_p(s) = \frac{as}{L}, \tag{60}$$

which satisfies

$$f_p(0) = 0, \quad f_p(L) = a. \tag{61}$$

The homogeneous part satisfies

$$f_h(s,t) = \sum_{n=1}^{\infty} C_n \sin\left(\frac{n\pi s}{L}\right) \sinh\left(\frac{n\pi t}{L}\right). \tag{62}$$

To satisfy $f(s,H) = g(s)$, we impose

$$g(s) - \frac{as}{L} = \sum_{n=1}^{\infty} C_n \sinh\left(\frac{n\pi H}{L}\right) \sin\left(\frac{n\pi s}{L}\right). \tag{63}$$

This is a Fourier sine series, so the coefficients C_n are given by

$$C_n = \frac{2}{L\sinh\left(\frac{n\pi H}{L}\right)} \int_0^L \left[g(s) - \frac{as}{L}\right] \sin\left(\frac{n\pi s}{L}\right) ds. \tag{64}$$

Final solution. Returning to the original variables, the solution is

$$f(x,y) = \frac{a}{L} s(x) + \sum_{n=1}^{\infty} C_n \sin\left(\frac{n\pi s(x)}{L}\right) \sinh\left(\frac{n\pi t(y)}{L}\right), \tag{65}$$

with the coefficients

$$C_n = \frac{2}{L\sinh\left(\frac{n\pi H}{L}\right)} \int_0^L \left[g(s) - \frac{as}{L}\right] \sin\left(\frac{n\pi s}{L}\right) ds. \tag{66}$$

It is important to highlight that we would have obtained the same result if we had used Theorem 4.

The Figure 1 presents a numerical solution to the conformable generalized Laplace equation with non-equal fractional orders, as defined in equation (51). In this case, the parameters were set to $\alpha_1 = 0.5$, $\alpha_2 = 0.75$, $p = 5$, and $q = 5$. The spatial modulation functions were given by $h_1(x,\ \alpha_1) = x^{1-\alpha_1}$ and $h_2(y,\ \alpha_2) = y^{1-\alpha_2}$ (the corresponding kernel functions are depicted in Figure 2, providing a visual reference for their spatial behavior and their role in the conformable derivative formulation). The solution surface, presented in Figure 1, exhibits a complex, oscillatory pattern characteristic of systems operating in an anisotropic medium. This anisotropy is introduced by the distinct fractional orders ($\alpha_1 = 0.5$ and $\alpha_2 = 0.75$), which cause a non-uniform spatial scaling. The resulting profile diverges significantly from the smooth, non-oscillatory solution expected from the classical integer-order Laplace equation, confirming the model's ability to capture local potential variations. This heterogeneous behavior is directly attributable to the spatially dependent kernel functions h_1 and h_2. These functions correspond to the classical conformable derivative in the sense of Khalil. The equation was subject to homogeneous Dirichlet boundary conditions along the edges $x = 0$, $x = p$, and $y = 0$, while a nonhomogeneous Dirichlet condition $f(x, q) = g(x) = \dfrac{2}{\sqrt{\pi}} e^{-x^2/2}$ was imposed along the upper boundary. To obtain the numerical solution, a structured uniform mesh of 100×100 grid points was employed to discretize the rectangular domain $[0,\ p] \times [0,\ q]$. The differential operator was approximated using second-order centered finite differences applied to the composite operators $({}^{h_1}P_x^{\alpha_1})^2$ and $({}^{h_2}P_y^{\alpha_2})^2$, and the resulting sparse linear system was solved using direct sparse solvers. The implementation was carried out in Python 3.13.8, utilizing the libraries `NumPy`, `SciPy`, and `Matplotlib` for numerical computation and visualization.

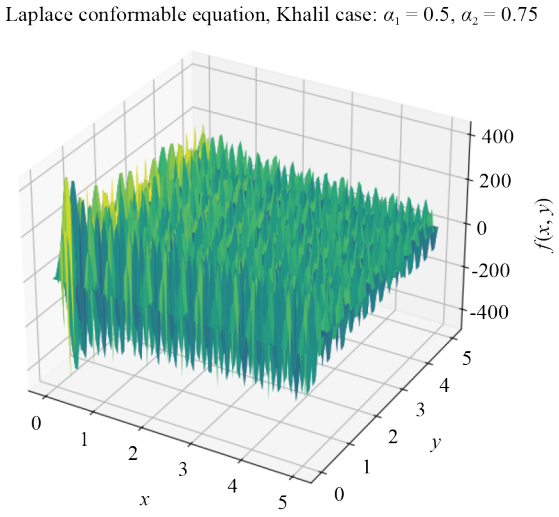

Figure 1. Three-dimensional numerical solution of the conformable generalized Laplace equation using Khalil's definition of the conformable derivative. Parameters: $\alpha_1 = 0.5$, $\alpha_2 = 0.75$, domain size $p = q = 5$, with Dirichlet boundary conditions. The solution is obtained via a finite difference method using a uniform grid and sparse matrix solvers

These functions correspond to the classical conformable derivative in the sense of Khalil. The equation was subject to homogeneous Dirichlet boundary conditions along the edges $x = 0$, $x = p$, and $y = 0$, while a nonhomogeneous Dirichlet condition $f(x, q) = g(x) = \dfrac{2}{\sqrt{\pi}} e^{-x^2/2}$ was imposed along the upper boundary. The solution surface, presented in Figure 1, exhibits a complex, oscillatory pattern characteristic of systems operating in an anisotropic medium, where the spatial scaling is non-uniform due to the distinct fractional orders $\alpha_1 = 0.5$ and $\alpha_2 = 0.75$. The resulting profile demonstrates that the conformable model effectively captures local variations in potential, diverging significantly from the smooth, non-oscillatory solution expected from the classical integer-order Laplace equation. This anisotropic behavior is directly traceable to the spatially dependent kernel functions h_1 and h_2, which introduce a non-linear scaling of the coordinates. To obtain the numerical solution, a structured uniform mesh of 100×100 grid points was employed to

discretize the rectangular domain $[0, p] \times [0, q]$. The differential operator was approximated using second-order centered finite differences applied to the composite operators $({}^{h_1}P_x^{\alpha_1})^2$ and $({}^{h_2}P_y^{\alpha_2})^2$, and the resulting sparse linear system was solved using direct sparse solvers. The implementation was carried out in Python 3.13.8, utilizing the libraries `NumPy`, `SciPy`, and `Matplotlib` for numerical computation and visualization.

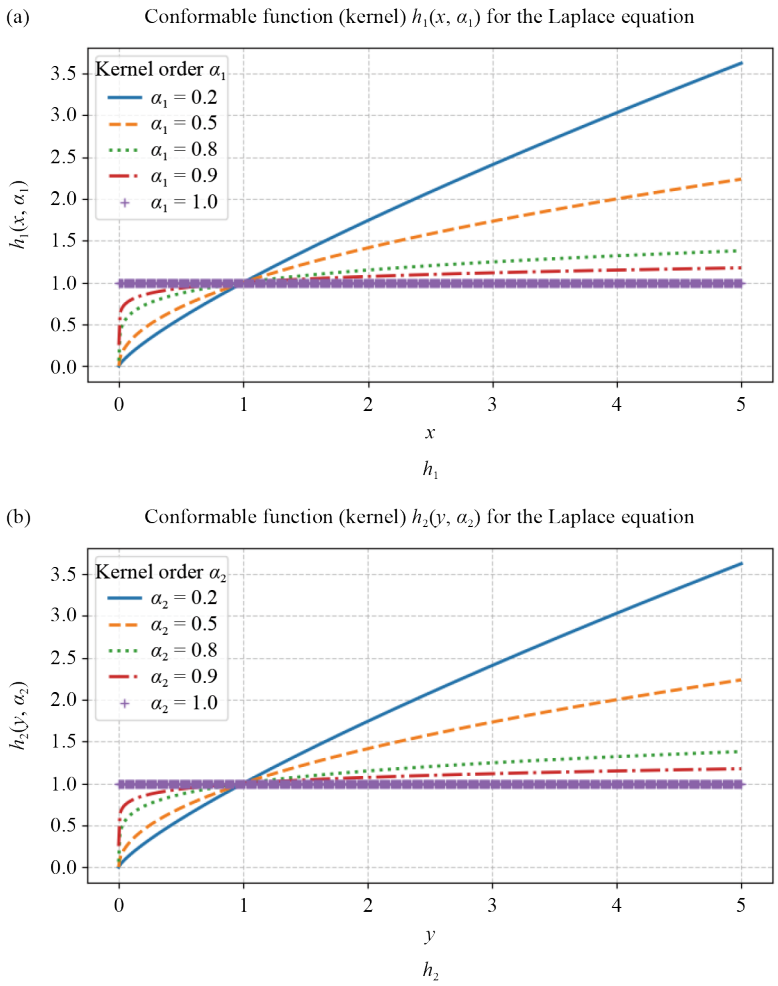

Figure 2. Conformable kernel functions h_1 and h_2 for the Laplace equation. The plots illustrate the singular behavior near the origin for fractional orders $0 < \alpha < 1$, demonstrating the smooth transition from classical to fractional kernels

In Figure 3, we present a collection of heat maps corresponding to numerical solutions of the generalized conformable Laplace equation. Each subfigure illustrates the behavior of the solution $f(x, y)$ under distinct combinations of fractional orders α_1 and α_2, where α_1 corresponds to the conformable derivative in the x-direction, and α_2 in the y-direction. The nine heat maps clearly demonstrate how the anisotropy, induced by the choice of α_1 and α_2, modulates the spatial pattern of the solution. When $\alpha_1 = \alpha_2 = 1.000$, the classical Laplace equation is recovered, showing a uniform and highly structured oscillatory behavior typical of separation of variables solutions in a classical domain. As either α_1 or α_2 decreases (e.g., the cases $\alpha_1 = 0.333$, $\alpha_2 = 1.000$ or $\alpha_1 = 1.000$, $\alpha_2 = 0.333$), the wave structure becomes stretched and less uniform in the corresponding dimension. For cases where both orders are fractional and unequal (e.g., $\alpha_1 = 0.333$, $\alpha_2 = 0.666$ or $\alpha_1 = 0.666$, $\alpha_2 = 0.333$), the solution exhibits complex, asymmetric wave patterns, confirming the ability of the generalized conformable derivative to model anisotropic and heterogeneous media. The color scale further reveals that

lower fractional orders generally lead to a solution profile with higher spatial amplitudes or a more pronounced oscillation near the boundaries, reflecting the local scaling effect of the conformable kernels.

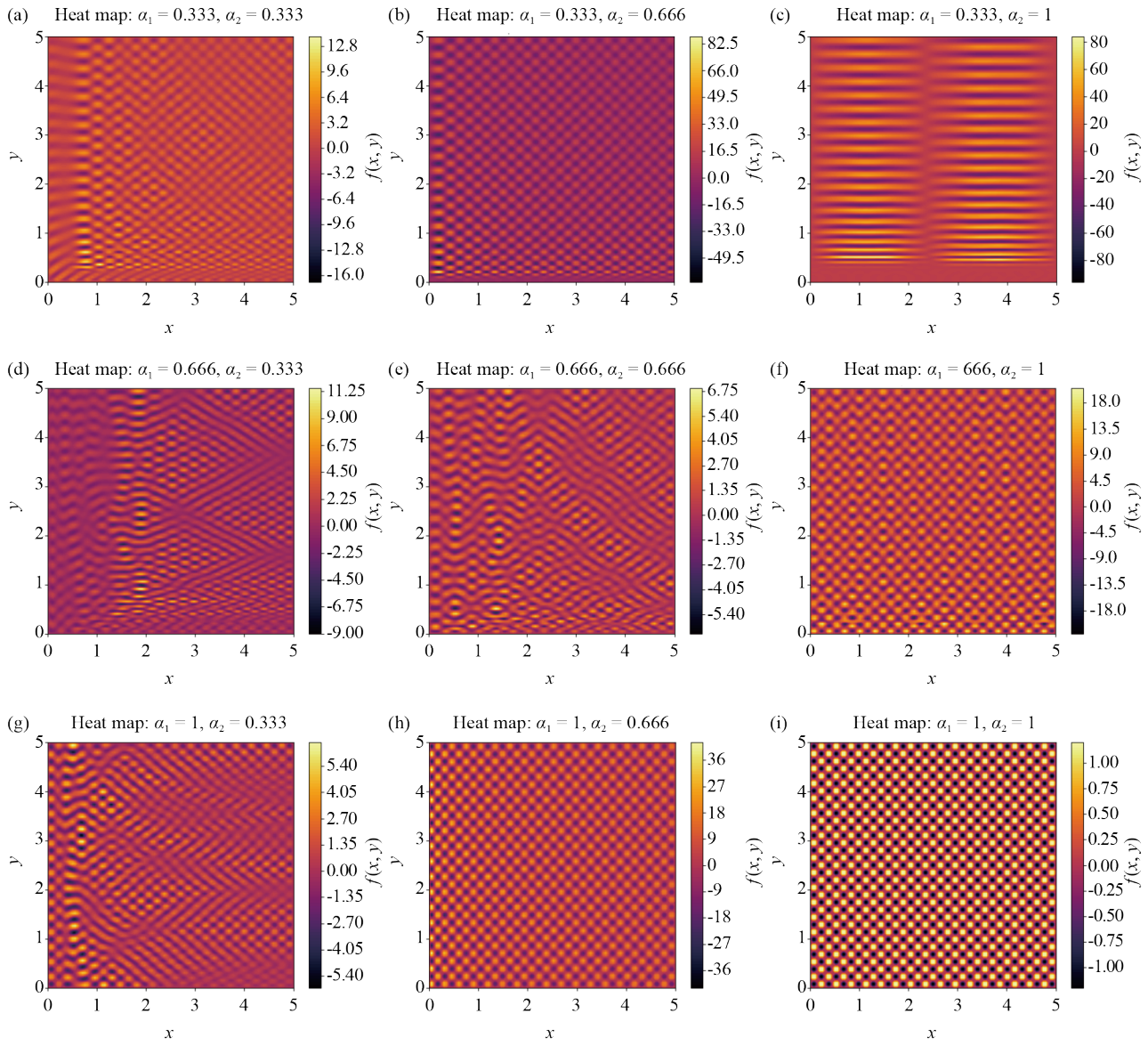

Figure 3. Heat maps of the solution $f(x, y)$ to the generalized conformable Laplace equation for different combinations of the fractional orders (α_1, α_2)

5.2 *Fokker-Planck equation*

The Fokker-Planck (FP) equation governs the spatio-temporal evolution of a probability-density function $u = u(x, t)$ associated with stochastic processes subject to both deterministic drift and random fluctuations. While traditional formulations employ second-order spatial derivatives, recent fractional approaches [19] have extended this framework to model subdiffusive behaviour through non-local operators and continuous-time random walk asymptotics. Our work presented a novel alternative using generalized conformable calculus that preserves the local structure of the differential operators while capturing anomalous transport through variable-order kernels. Unlike fractional methods that require solution mapping through integral transforms, our conformable formulation maintains direct physical interpretation of

both drift and diffusion terms, with the added capability of modeling position and time-dependent anomalous effects through carefully designed kernel functions. This approach proves particularly valuable for systems where the transport anomalies stem from local material heterogeneities rather than purely non-local dynamics.

In its classical form the diffusive term is a second-order derivative in x; here, by contrast, we consider the variant

$$\frac{\partial u}{\partial t} = \frac{\partial}{\partial x}\left[\left(\frac{\partial u}{\partial t} + x\right) u\right], \tag{67}$$

supplemented with the Dirac-delta initial datum

$$u(x, 0) = \delta\big(x - x_0\big), \quad x_0 \in \mathbb{R}. \tag{68}$$

5.2.1 *Physical interpretation*

Equation (67) prescribes a probability flux that depends explicitly on the instantaneous rate of change u_t. This non-standard coupling produces a *memory-like* mechanism: the spatial transport at time t is modulated by the present temporal evolution of the density, thereby modelling anomalous diffusion phenomena that cannot be captured by a purely spatial Laplacian [20, 21].

For the Fokker-Planck equation given by (67), the spatial variable is $x \in \mathbb{R}$, and the time variable is $t \in \mathbb{R}^+$. The unknown function $u(x, t)$ represents the Probability Density Function (PDF) that describes the spatio-temporal evolution of particles. x_0 is the initial position of the particles, constrained to $x_0 \in \mathbb{R}$.

5.2.2 *Conformable generalisation*

Replacing the ordinary derivatives in (67) with conformable derivatives of orders $0 < \alpha_1, \alpha_2 \leq 1$ yields

$${}^{h_2}P_t^{\alpha_2} u(x, t) = {}^{h_1}P_x^{\alpha_1}\left[\big({}^{h_2}P_t^{\alpha_2} u(x, t) + x\big) u(x, t)\right], \tag{69}$$

which, after expanding each conformable operator as $h(t, \alpha)\partial/\partial t$ or $h(x, \alpha)\partial/\partial x$, is equivalent to

$$h_2(t, \alpha_2)\, u_t = h_1(x, \alpha_1)\, \frac{\partial}{\partial x}\left[\big(h_2(t, \alpha_2)\, u_t + x\big) u\right], \tag{70}$$

where the kernels

$$h_1(x, \alpha_1) = \big(1.001 + \sin 2\pi x\big)^{1-\alpha_1}, \tag{71}$$

$$h_2(t, \alpha_2) = \big(1.001 + \cos 2\pi t\big)^{1-\alpha_2}, \tag{72}$$

are C^1, strictly positive, and oscillatory, thereby inducing an additional spatial-temporal modulation (the corresponding kernel functions are illustrated in Figure 4, providing a visual depiction of their periodic behavior and modulation effects).

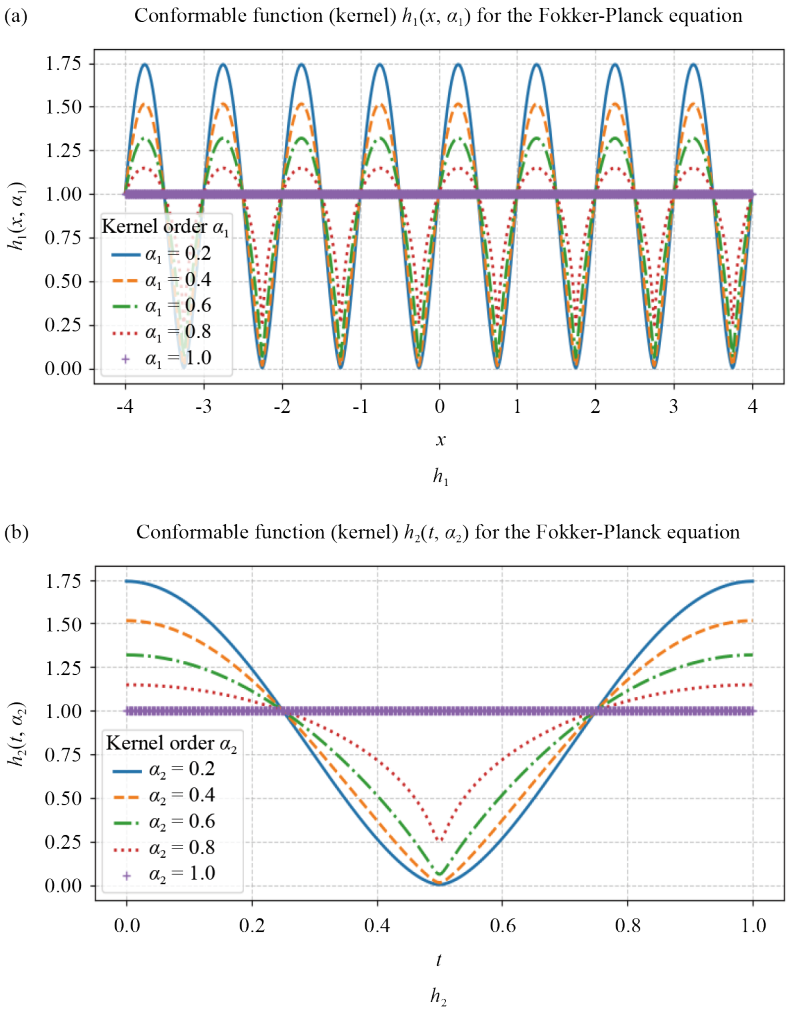

Figure 4. Conformable kernel functions h_1 and h_2 for the Fokker-Planck equation. The figures illustrate the periodic scaling behavior of the kernels, ensuring strictly positive values and reflecting localized anomalous structures

5.2.3 *Analytic solution*

Solving (67)-(68) via the transformation $\xi = xe^t$, $\sigma = \dfrac{1}{2}(e^{2t} - 1)$ produces the Gaussian profile

$$u(x, t) = \frac{e^t}{\sqrt{2\pi\left(e^{2t} - 1\right)}} \exp\left[-\frac{(xe^t - x_0)^2}{2\left(e^{2t} - 1\right)}\right]. \tag{73}$$

Substituting the conformable integrals ${}^{h_1}_{a_1}I^{\alpha_1}_x$ and ${}^{h_2}_{a_2}I^{\alpha_2}_t$ for x and t in (73) yields the explicit conformable density

$$u\left({}^{h_1}_{a_1}I^{\alpha_1}_x,\ {}^{h_2}_{a_2}I^{\alpha_2}_t\right) = \frac{\exp\left({}^{h_2}_{a_2}I^{\alpha_2}_t\right)}{\sqrt{2\pi\left(\exp[2\,{}^{h_2}_{a_2}I^{\alpha_2}_t] - 1\right)}} \exp\left[-\frac{\left({}^{h_1}_{a_1}I^{\alpha_1}_x \exp\left({}^{h_2}_{a_2}I^{\alpha_2}_t\right) - x_0\right)^2}{2\left(\exp[2\,{}^{h_2}_{a_2}I^{\alpha_2}_t] - 1\right)}\right]. \tag{74}$$

5.2.4 *Numerical ilustration*

Figure 5 displays the heat maps of $u(x, t)$ computed from (74) for the four representative values $\alpha = \alpha_1 = \alpha_2 \in \{0.25, 0.50, 0.75, 1.00\}$. The panels reveal two salient features.

1. Temporal spread: As α decreases, the effective diffusion slows down, producing broader probability "plumes" that persist for longer times (compare Figures 5d and 5a).

2. Oscillatory modulation: Owing to the trigonometric form of the kernels h_1 and h_2, small amplitude spatial oscillations emerge in all conformable cases; their intensity grows as α departs from the classical value 1. These ripples, clearly visible in Figures 5a-5c, are a direct manifestation of the non-uniform weights embedded in the conformable operators.

Such behaviour underscores the flexibility of the conformable formalism: by a judicious choice of kernel one can encode spatial or temporal heterogeneity, memory, and even mild oscillatory patterns while retaining an analytic handle on the solution.

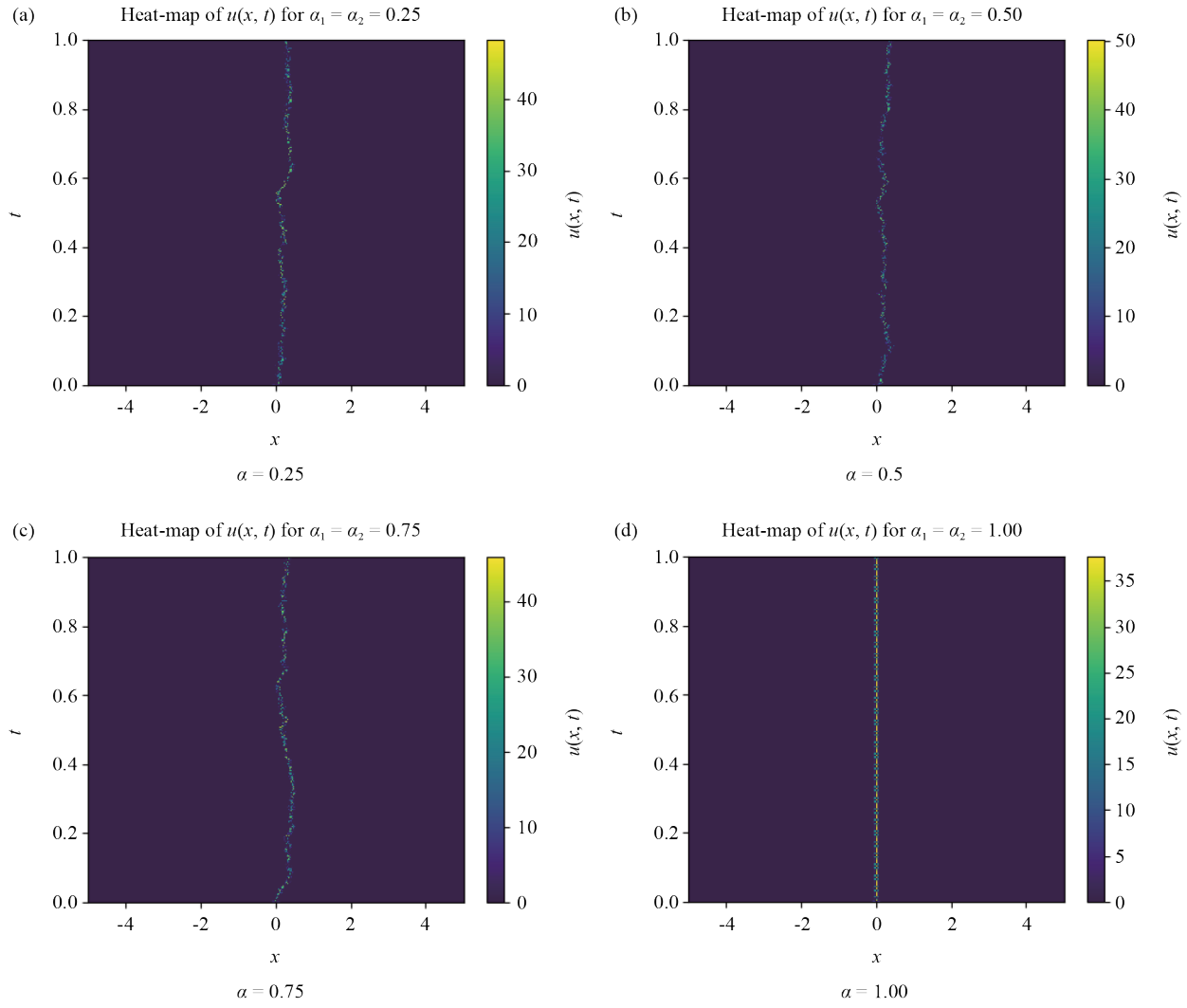

Figure 5. Heat maps of the Fokker-Planck density $u(x, t)$ for four conformable orders $\alpha = \alpha_1 = \alpha_2$. Oscillatory structures caused by the kernels h_1 and h_2 become more pronounced as α decreases

To illustrate the effects of non-symmetric conformable orders in space and time, we present in Figure 6 several heat maps of the Fokker-Planck density $u(x, t)$ for different combinations of $\alpha_1 \neq \alpha_2$. These heat maps vividly demonstrate the strong influence of the non-symmetric fractional orders (α_1, α_2) on the diffusion profile of the probability density $u(x, t)$. The parameter α_1 governs the temporal scaling, while α_2 controls the spatial scaling. In the scenario where the temporal order is extremely small ($\alpha_1 = 0.01$) and the spatial order is classical ($\alpha_2 = 1$), the density profile exhibits an exceptionally rapid decay, appearing almost instantaneously across the spatial domain, which is consistent with a hyper-diffusive process in the time variable. Conversely, when the temporal order is classical ($\alpha_1 = 1$) and the spatial order is very small ($\alpha_2 = 0.01$), the density evolves much slower over time but maintains a high degree of spatial concentration, resembling a highly localized front. The intermediate asymmetric cases (for instance, $\alpha_1 = 0.75$, $\alpha_2 = 0.25$ and $\alpha_1 = 0.25$, $\alpha_2 = 0.5$) display transitional behavior, where the relative dominance between the temporal and spatial fractional orders dictates the resulting shape and spread velocity of the diffusion profile. Specifically, the strong spatial-temporal anisotropy leads to significant variations in the width, amplitude, and overall propagation speed of the diffusion front.

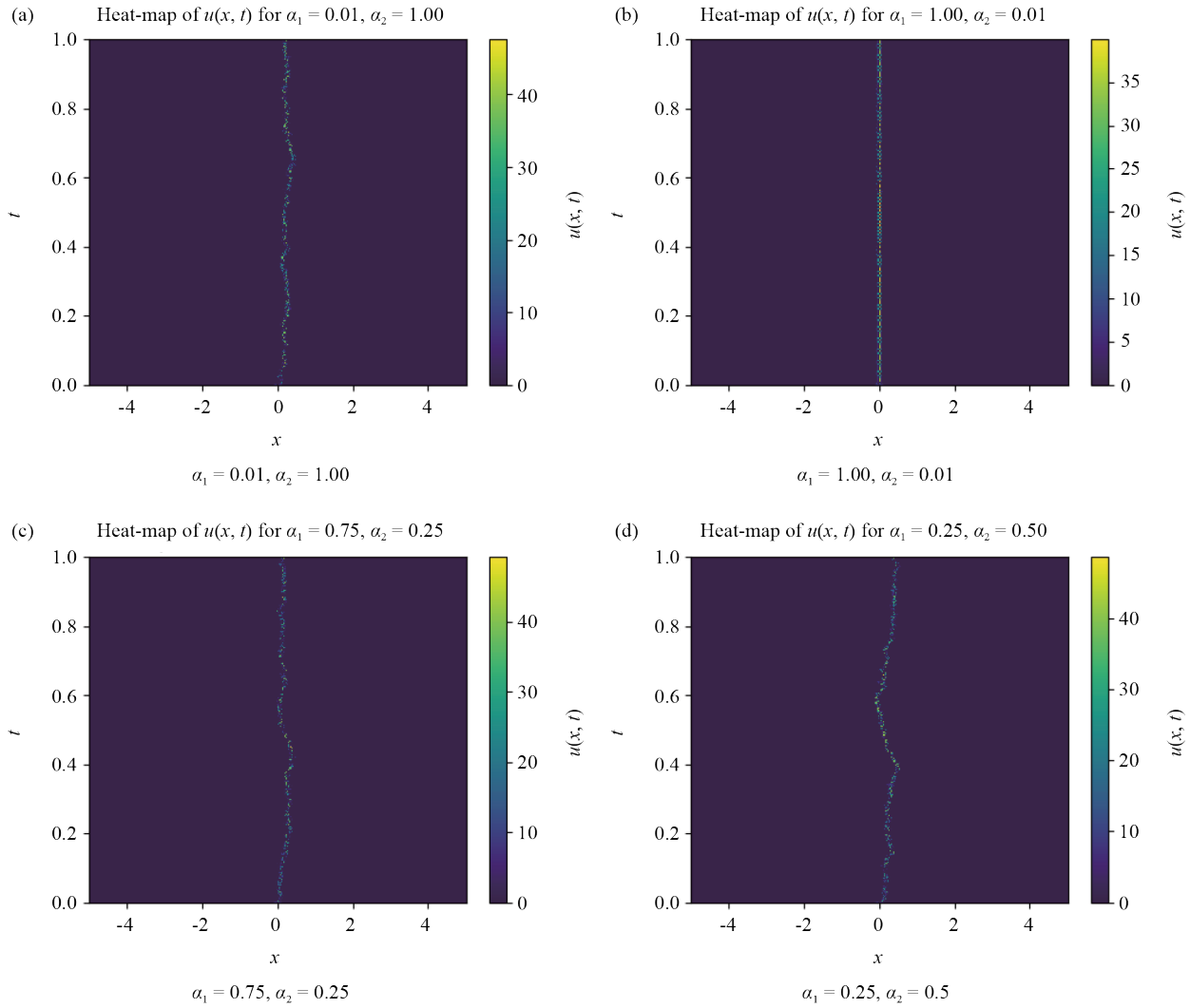

Figure 6. Heat maps of the Fokker-Planck density $u(x, t)$ for four asymmetric combinations of conformable orders $(\alpha_1 \neq \alpha_2)$. The anisotropy introduced by different time and space fractionalities leads to notable variations in the diffusion profile

The numerical evidence presented in Figure 5 was obtained with a Python implementation of an explicit up-wind finite-difference scheme, using Python 3.13.8. The spatial domain $x \in [-5, 5]$ was discretised with $N_x = 800$ nodes ($\Delta x \approx 1.25 \times 10^{-2}$), whereas the temporal interval $t \in [0, 1]$ employed $N_t = 2{,}000$ steps ($\Delta t = 5 \times 10^{-4}$), values that satisfy the customary stability requirement $\Delta t \lesssim \frac{1}{2}\Delta x^2$. The initial Dirac delta was approximated by a narrow Gaussian of variance $\sigma_0^2 = 5 \times 10^{-3}$, and absorbing boundaries were enforced at $x = \pm 5$. At every time level the scheme renormalises the solution to unity, thereby preserving the total probability. Four simulations were conducted for the conformable orders $\alpha = \alpha_1 = \alpha_2 \in \{0.25, 0.50, 0.75, 1.00\}$; each run produced a two-dimensional heat map rendered with the `viridis` colour map, whose captions indicate the common value of α. The code excerpt reproduced above fully specifies the solver, the kernel definitions, and the post-processing routines used to generate the visualisations [22]. The results presented in Figure 5 demonstrate the dependency of the diffusion process on the identical and coupled spatial and temporal fractional orders. As the order α decreases from the classical case ($\alpha = 1.00$), the solution profile deviates significantly from the standard Gaussian diffusion expected for integer-order systems. The density distribution exhibits increasingly pronounced oscillatory structures. Lower values of α (e.g., $\alpha = 0.25$) intensify these localized fluctuations, indicating that the effective local diffusion coefficient becomes highly anisotropic and position-dependent, showcasing the capacity of the generalized conformable derivative to model anomalous diffusion phenomena characterized by localized heterogeneity.

5.3 *Generalized conformable wave equation*

The wave equation represents a fundamental model for understanding propagation phenomena across physics and engineering. While traditional studies focus on integer-order derivatives, recent advances have explored fractional-order formulations [23], which exhibit unique non-local properties and modified dispersion characteristics. In this section, we present a generalized conformable alternative for two-dimensional wave propagation (one spatial and one temporal dimension), offering distinct advantages over fractional approaches. Our conformable framework maintains local operator properties while capturing essential anomalous propagation effects through carefully designed kernel functions. This approach provides a mathematically tractable yet physically meaningful alternative to fractional models, particularly suitable for systems where the propagation medium exhibits position and time-dependent properties that can be encoded in the conformable kernels.

We consider the generalized wave equation in conformable form

$$\left({}^{h_1}P_t^{\alpha_1}\right)^2 u(x,t) = c^2 \left({}^{h_2}P_x^{\alpha_2}\right)^2 u(x,t),$$

$$\left(h_1(t,\alpha_1)\frac{\partial}{\partial t}\right)^2 u(x,t) = c^2 \left(h_2(x,\alpha_2)\frac{\partial}{\partial x}\right)^2 u(x,t), \tag{75}$$

$$h_1^2(t,\alpha_1)\frac{\partial^2 u}{\partial t^2} + h_1(t,\alpha_1)\frac{\partial h_1}{\partial t}(t,\alpha_1)\frac{\partial u}{\partial t} = c^2\left[h_2^2(x,\alpha_2)\frac{\partial^2 u}{\partial x^2} + h_2(x,\alpha_2)\frac{\partial h_2}{\partial x}(x,\alpha_2)\frac{\partial u}{\partial x}\right],$$

with boundary and initial conditions

$$u(0,t) = 0, \quad u(L,t) = 0, \quad t \geq 0, \tag{76}$$

$$u(x,0) = f(x), \tag{77}$$

$$\left.\frac{\partial u}{\partial t}\right|_{t=0} = g(x), \quad x \in (0, L). \tag{78}$$

For the generalized conformable wave equation (75): $u(x,t)$ represents the displacement of the wave, c is the constant wave speed, and L is the length of the spatial domain. The parameters α_1 and α_2 are the temporal and spatial fractional orders, respectively, with $\alpha_1,\ \alpha_2 \in (0,\ 1]$. $h_1(t,\ \alpha_1)$ and $h_2(x,\ \alpha_2)$ are the strictly positive, continuously differentiable temporal and spatial kernel functions, which modulate the local speed and spatial scaling of the wave. $f(x)$ and $g(x)$ are the initial displacement and initial velocity functions, respectively.

Change of variables. We define the following change of variables

$$s(x) = \int_0^x \frac{d\xi}{h_2(\xi,\ \alpha_2)}, \quad \tau(t) = \int_0^t \frac{d\theta}{h_1(\theta,\ \alpha_1)}, \tag{79}$$

and so

$$s(0) = 0, \quad s(L) = P, \quad \tau(0) = 0, \quad \tau(T) = Q. \tag{80}$$

Under this transformation, the PDE becomes the classical wave equation

$$\frac{\partial^2 u}{\partial \tau^2} = c^2 \frac{\partial^2 u}{\partial s^2}, \tag{81}$$

with new domain and conditions

$$u(0,\ \tau) = 0, \quad u(P,\ \tau) = 0, \tag{82}$$

$$u(s,\ 0) = \tilde{f}(s), \tag{83}$$

$$\left.\frac{\partial u}{\partial \tau}\right|_{\tau=0} = \tilde{g}(s), \tag{84}$$

where $\tilde{f}(s) = f(x(s))$, and similarly $\tilde{g}(s) = g(x(s))$.

Solution via separation of variables. We look for a solution of the form

$$u(s,\ \tau) = \sum_{n=1}^{\infty} \left[A_n \cos\left(\frac{n\pi c\tau}{P}\right) + B_n \sin\left(\frac{n\pi c\tau}{P}\right)\right] \sin\left(\frac{n\pi s}{P}\right). \tag{85}$$

Using the orthogonality of sine functions, we compute the coefficients

$$A_n = \frac{2}{P}\int_0^P \tilde{f}(s)\sin\left(\frac{n\pi s}{P}\right)ds, \tag{86}$$

$$B_n = \frac{2}{n\pi c}\int_0^P \tilde{g}(s)\sin\left(\frac{n\pi s}{P}\right)ds. \tag{87}$$

Final solution. Returning to the original variables, we obtain

$$u(x,t) = \sum_{n=1}^{\infty}\left[A_n\cos\left(\frac{n\pi c\,\tau(t)}{P}\right) + B_n\sin\left(\frac{n\pi c\,\tau(t)}{P}\right)\right]\sin\left(\frac{n\pi s(x)}{P}\right), \tag{88}$$

with the transformed coordinates

$$s(x) = \int_0^x \frac{d\xi}{h_2(\xi,\,\alpha_2)}, \qquad \tau(t) = \int_0^t \frac{d\theta}{h_1(\theta,\,\alpha_1)}. \tag{89}$$

The coefficients A_n, B_n are

$$A_n = \frac{2}{P}\int_0^P f(s)\sin\left(\frac{n\pi s}{P}\right)ds, \tag{90}$$

$$B_n = \frac{2}{n\pi c}\int_0^P g(s)\sin\left(\frac{n\pi s}{P}\right)ds. \tag{91}$$

In Figure 7, we present the numerical solution of the one-dimensional generalized conformable wave equation. The parameters and initial conditions were chosen as follows: $f(x) = \sin\left(\frac{\pi x}{L}\right)$, $g(x) = 0$, and $L = 1$. The conformable coefficients are given by $h_1(t,\ \alpha_1) = e^{(1-\alpha_1)\sin(t)}$ and $h_2(x,\ \alpha_2) = e^{(1-\alpha_2)\cos(x)}$, with $\alpha_1,\ \alpha_2 \in \{1/4,\ 1/2\}$ (the corresponding kernel functions are depicted in Figure 8, providing a visual reference for their temporal and spatial behavior). These functions ensure a dimensionless formulation compatible with conformable derivative theory. The resulting plots illustrate the wave propagation dynamics within this generalized fractional framework. The four plots in Figure 7 demonstrate how the non-constant temporal (α_1) and spatial (α_2) scalings affect the wave solution. When the fractional orders are identical ($\alpha_1 = \alpha_2 = 0.25$ or $\alpha_1 = \alpha_2 = 0.5$), the wave propagation appears relatively more coherent and symmetric compared to the anisotropic cases. Specifically, in the fully fractional case ($\alpha_1 = 0.25,\ \alpha_2 = 0.25$), the solution exhibits higher initial amplitude and faster decay, suggesting that lower orders increase the effective wave speed or amplitude within the conformable metric. For the asymmetric cases (e.g., $\alpha_1 = 0.25$, $\alpha_2 = 0.5$ and $\alpha_1 = 0.5$, $\alpha_2 = 0.25$), a clear anisotropy is observed, where the temporal and spatial modulations dictate the rate of dispersion and the localized shape of the wave packet. The differences in peak height and spatial-temporal spreading between the various combinations confirm that the generalized conformable framework successfully captures heterogeneous propagation effects.

The numerical solutions presented in Figure 7 are obtained through a Python implementation using NumPy and Matplotlib (Python 3.13.8) that solved the generalized conformable wave equation using an explicit finite-difference scheme. The spatial domain is discretized with $x \in [0,\ 1]$ using $N_x = 100$ nodes ($\Delta x = 0.01$) while the temporal domain $t \in [0,\ 2]$ employed $N_t = 100$ steps ($\Delta t = 0.02$), parameters that satisfy the Courant Friedrichs Lewy (CFL) stability condition $\Delta t \leq \Delta x/c$ for the chosen wave speed $c = 1$. The initial conditions are set as $u(x,\ 0) = \sin(\pi x/L)$ for the

displacement field and $\partial_t u(x,0) = 0$ for the initial velocity, with fixed boundary conditions $u(0,t) = u(L,t) = 0$ maintained throughout the simulation.

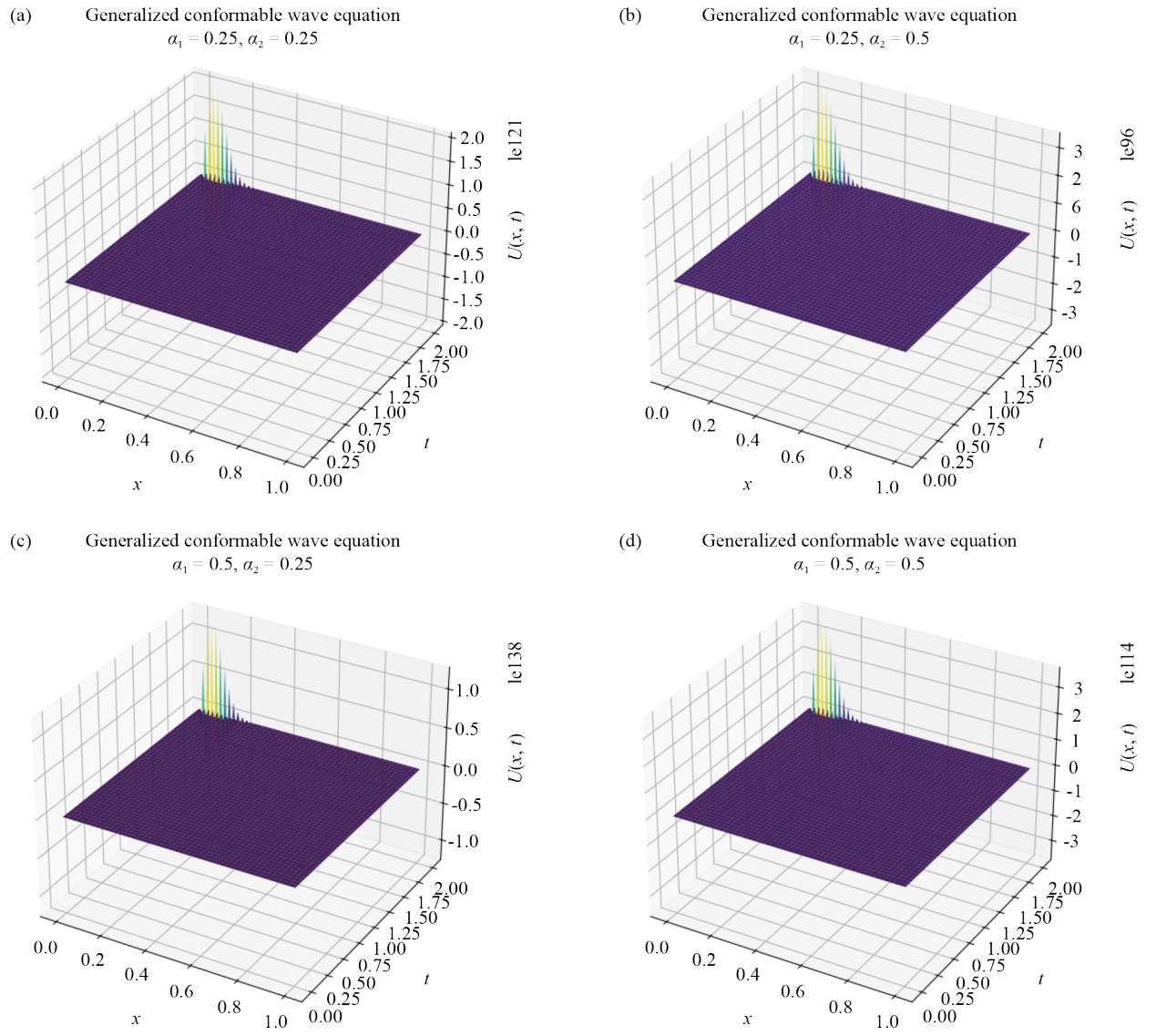

Figure 7. Thermal maps for the generalized conformable wave equation for selected conformable orders $\alpha_1, \alpha_2 \in \{0.25, 0.5\}$

The conformable nature of the equation is implemented through the kernel functions $h_1(t, \alpha_1) = e^{(1-\alpha_1)\sin t}$ for temporal derivatives and $h_2(x, \alpha_2) = e^{(1-\alpha_2)\cos x}$ for spatial derivatives, with their respective derivatives $\partial h_1/\partial t = (1-\alpha_1)\cos t \cdot h_1(t, \alpha_1)$ and $\partial h_2/\partial x = -(1-\alpha_2)\sin x \cdot h_2(x, \alpha_2)$ computed analytically. The numerical scheme employed a predictor-corrector approach to handle the nonlinear coupling introduce by these conformable terms, incorporating a small regularization parameter $\varepsilon = 10^{-8}$ to prevent division by zero in regions where kernel values became extremely small. Solutions are computed for all combinations of conformable orders $\alpha_1, \alpha_2 \in \{0.25, 0.5\}$, with the resulting wave propagation patterns visualized as three-dimensional surface plots using Matplotlib's `viridis` colormap to highlight the characteristic distortions induced by different combinations of spatial and temporal conformable orders.

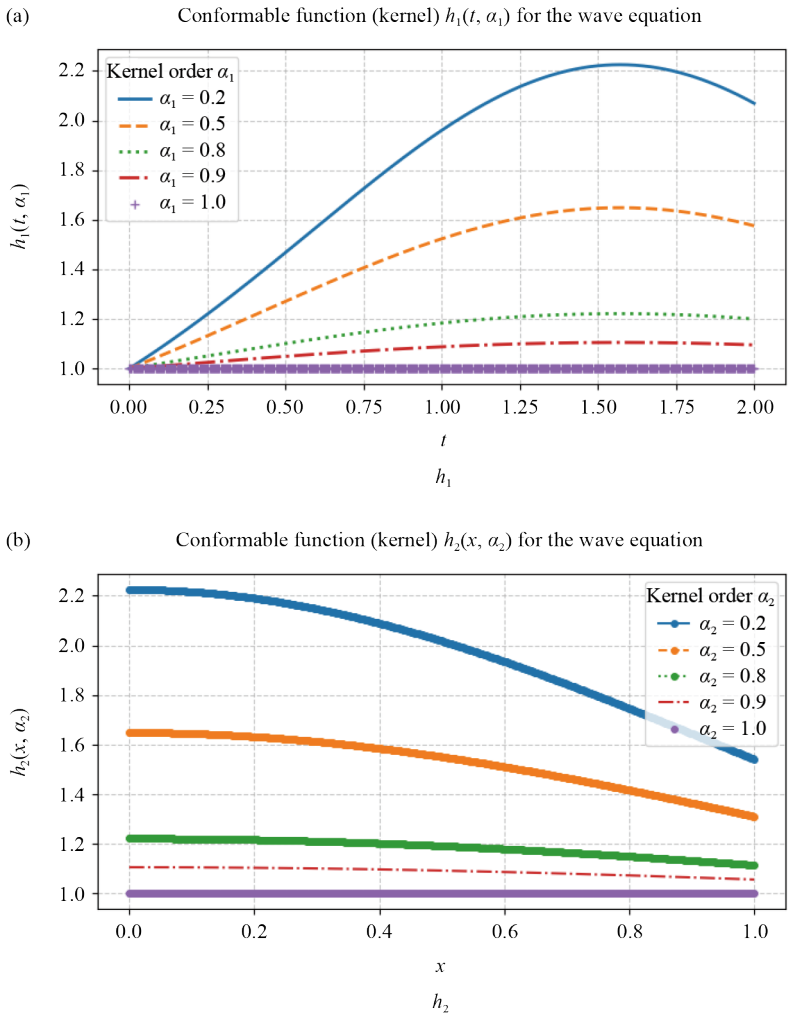

Figure 8. Conformable kernel functions h_1 and h_2 for the wave equation. The visualizations highlight the oscillatory behavior induced by the exponential-trigonometric kernel forms across the specified intervals

6. Discussion

The findings reported herein demonstrate that the *generalised conformable derivative* constitutes a mathematically sound and physically meaningful extension of classical differential operators for modelling anomalous transport. By proving an explicit coordinate equivalence between the standard second-order linear partial differential equation (17) and its conformable counterpart (18), we establish that the new operator family does not modify the intrinsic differential order; instead, it embeds the dynamics in a metric that is locally rescaled by the smooth, strictly positive kernels h_1 and h_2. This observation is crucial because it implies that many analytical tools of conventional theory, such as maximum principles, energy estimates, and comparison theorems, remain valid in the conformable setting, provided the kernels satisfy the regularity hypotheses spelled out in the Lemma 1. In practical terms, one may therefore transfer well-known solution methods, stability criteria, and numerical schemes almost verbatim to the conformable framework.

A second, equally important implication of the coordinate correspondence is the so-called solution-transfer principle: any closed-form solution of the reference equation can be mapped into a solution of the conformable-generalised equation by the mere substitution of ordinary integrals with conformable integrals. In particular, the analytic Gaussian density (73) that solves the modified Fokker-Planck equation (67)-(68) is converted into its conformable analogue (74) without altering its functional structure. This property markedly distinguishes the conformable approach from most fractional models,

whose solutions typically involve special functions of Mittag-Leffler or Fox-W type and are therefore less accessible for analytical or computational manipulation.

The physical interpretation of the conformable kernels emerges naturally from this perspective. Because each kernel multiplies an ordinary derivative, it plays the role of a *local stretch factor* that contracts or dilates the effective spatial or temporal metric. In the illustrative example of the Fokker-Planck equation, the oscillatory choices $h_1(x,\,\alpha) = (1.001 + \sin 2\pi x)^{1-\alpha}$ and $h_2(t,\,\alpha) = (1.001 + \cos 2\pi t)^{1-\alpha}$ induce periodic modulation of the diffusion coefficient. Consequently, the probability density exhibits alternating phases of accelerated and retarded spreading, which manifest in the heat maps (Figure 5) as mild oscillations around the main Gaussian ridge. These features illustrated how conformable derivatives encoded heterogeneous media or time-dependent memory effects while preserving the essential structure of the governing equation.

The conformable wave equation analysis in section 5.3 demonstrates how the framework captures anisotropic wave propagation through distinct spatial and temporal conformable orders ($\alpha_1 \neq \alpha_2$). The numerical solutions reveal characteristic wavefront distortions and velocity modifications, particularly when $\alpha_1 < \alpha_2$, suggesting applications in graded metamaterials. Crucially, the transformation preserves the equation's hyperbolic character while introducing kernel-controlled scaling of wave parameters.

The conformable Laplace equation study in section 5.1 provides insights into boundary value problems with position-dependent properties. The solutions demonstrated how sub-unity orders ($\alpha < 1$) generate smoothed potential fields while maintaining harmonic properties, offering a powerful tool for modeling anisotropic media in electrostatics and heat conduction problems through physically interpretable kernel functions.

Our numerical experiments further reveal the quantitative influence of the conformable order α. When α approached unity, the kernels converged to one, and the dynamics reduced smoothly to the classical Fokker-Planck behaviour. As α decreases, the amplitudes of the kernel increase, amplifying the metric distortions and, thus, enhanced the oscillatory behaviour of the density. Importantly, the simulations confirm mass conservation and non-negativity of the solution, validated the finite-difference scheme derived from the weighted formulation (70). These observations suggest that conformable models may offer a controlled way of interpolating between classical diffusion and strongly anomalous regimes without sacrificing mathematical rigour or numerical stability.

The generalized conformable framework demonstrates a distinct advantage over classical fractional methods in scenarios demanding high modeling flexibility without sacrificing the analytical rigor of the local operator. For measuring anomalous heat transfer, our approach allows for the precise modeling of energy diffusion in metamaterials and heterogeneous media (where conductivity strongly depends on position or temperature), as demonstrated in prior work on operational temperature optimization in turbines [17]. Here, the kernel function can be meticulously tuned to reflect the physical, often anisotropic, structure of the medium—a challenge that traditional integral fractional operators often oversimplify by imposing a uniform non-local memory. This adaptability is key to modeling composite materials and layered systems where properties change abruptly.

Specifically, the method excels in:

• Anomalous Momentum Transfer in non-Newtonian fluids or complex polymer solutions, where the viscosity is dependent on a non-classical rate of deformation.

• Anomalous Mass Transfer in adsorption-desorption processes in porous media, such as pollutant migration in aquifers or diffusion across biological membranes.

• Wave Propagation in Structured Metamaterials, where the conformable derivative models the frequency-dependent effective mass or permittivity, accounting for structural heterogeneity that modifies the wave speed and dispersion relation locally.

• Financial Market Dynamics, where the kernel can be employed to model effective time or business time, adjusting the Black-Scholes equations to capture market "memory" effects locally.

The added value of the conformable transformation is its ability to convert these complex, kernel-dependent, anomalous transport models into standard, integer-order PDEs. This allows for the use of stable and well-established numerical and analytical tools, overcoming the significant computational burden often associated with integral fractional formulations.

Notwithstanding these promising results, several limitations warrant consideration. The present analysis is confined to linear partial differential equations of two variables and second order, leaving open the question of how nonlinearities might interact with the kernel-weighted operators. Specifically, the core strength of this method, the linearizing variable change $dt^* = h(t, \alpha)dt$, generally does not simplify or remove non-linear terms $N(u)$, often resulting in a new, time-dependent nonlinear system $\frac{du}{dt^*} = N(u)/h(t, \alpha)$. Furthermore, the requirement for smooth, strictly positive kernels excludes potentially interesting cases involving discontinuous or degenerate weighting functions. Finally, the physical interpretation of the kernels, while intuitive, requires empirical validation through comparison with experimental data in specific application domains.

Future research directions emerging from these limitations include the central objective of extending the framework to new families of nonlinear partial differential equations that satisfy the necessary transformation properties. Following an inductive reasoning approach, we aim to extend the analysis from two variables/second order to generalized systems of order n and m variables, as posited in the final conjecture of this work. Further research will also investigate singular or degenerate kernels, and develop systematic methodologies for kernel calibration from observational data. Such advances would further solidify the conformable approach as a versatile tool for modeling complex physical systems.

Taken together, the theoretical results and computational evidence advocated the conformable-generalised framework as a compelling alternative to traditional fractional calculus for problems in which analytic tractability, structural preservation, and physical interpretability are paramount. Future work would address the extension to nonlinear equations, the derivation of maximum-entropy principles under conformable dynamics, and the systematic calibration of kernel functions from experimental data in complex transport phenomena.

7. Conclusions

The present work puts forward a coherent framework for translating classical linear Partial Differential Equations (PDEs) into a *generalised conformable* setting through a carefully crafted coordinate transformation. The key idea is that any twice continuously differentiable solution of a second-order PDE is reformulated in terms of weighted first-order operators whose weights encode the conformable kernels h_1 and h_2. This seemingly modest observation leads to a set of powerful consequences. First, the analytical structure of the original equation, linearity, order, and boundary-value character, is preserved, while additional flexibility is introduced via the parameters $\alpha_1, \alpha_2 \in (0, 1]$. Second, the method avoids the heavy tails and non-local memory inherent to traditional fractional derivatives, thereby admitting classical solution techniques and standard numerical discretisations.

A significant advantage of the generalized conformable calculus combined with variable transformations lies in its ability to provide a mathematically rigorous bridge between classical and fractional frameworks while maintaining computational tractability. This approach enables the direct application of well-established analytical methods from classical PDE theory to conformable fractional equations, including separation of variables, Fourier analysis, and similarity transformations. The transformation methodology preserves the physical interpretability of solutions while introducing the flexibility to model complex phenomena such as anisotropic diffusion, heterogeneous media, and non-standard wave propagation through carefully designed kernel functions. Furthermore, the local nature of conformable derivatives ensures that numerical implementations remain computationally efficient compared to traditional fractional calculus approaches, making our framework particularly suitable for practical engineering applications and large-scale simulations.

The theoretical reach of the framework is illustrated with a modified Fokker-Planck equation whose diffusive flux depends explicitly on the instantaneous time derivative of the density. The conformable mapping yields a closed-form Gaussian solution in which the kernels appear only as smooth deformations of time and space. Heat-map simulations for representative kernel orders $\alpha = 0.25, 0.50, 0.75, 1.00$ reveal that lower α values introduce pronounced oscillations; these arise from the oscillatory nature of the chosen kernels and would not be captured by classical FP theory. Importantly, mass conservation and positivity remained intact, supporting the physical plausibility of the model.

Two limitations had to be acknowledged: (i) The current analysis was confined to *linear* equations; nonlinearities can interact non-trivially with the kernel weights, complicating both existence proofs and numerical stability. (ii) The conformable kernels are assumed smooth and strictly positive; degeneracy or discontinuity may invalidate the invertibility of the coordinate map and hence the equivalence results.

Several avenues for future work emerged naturally. One direction is the systematic identification or learning of kernel functions from experimental data, thereby tailoring conformable models to specific heterogeneous media. Another was the construction of high-order, kernelaware finite-difference schemes that maintain the favourable stability properties observed here. A third line of inquiry is the extension to systems of coupled PDEs, where distinct kernels might encode disparate physical processes such as reaction, advection, and diffusion.

Beyond the Fokker-Planck setting, the proposed conformable methodology is equally applicable to canonical PDEs such as the Laplace and wave equations. Given their foundational role in science and engineering, it is essential to highlight how these equations can be recast under a conformable framework. Introducing a fractional order via the generalised conformable derivative enriches the underlying dynamics and reveals anomalous features that are not present in the classical formulations. Sections 5.1 and 5.3 illustrate this capability by showing how conformable kernels enable a controlled deformation of space and time that preserves analytical structure while captures non-standard propagation and diffusion effects.

Although the conformable approach does not encode memory in the traditional fractional sense, it allows for localized variability in the PDE response by tuning the kernel exponents α. This property is particularly valuable when modeling systems that exhibit non-conventional or transitional dynamics, such as spatial inhomogeneities or time-dependent transport rates. The conformable calculus thus serves as a middle ground between classical and fully fractional models, offering both analytical tractability and the ability to capture essential features of anomalous diffusion and wave behavior.

Conjectural outlook. Let ${}^{h}L_m$ denote a linear partial differential operator of even order $m \geq 2$ in the generalized conformable framework, defined with smooth coefficients and appropriate conformable kernel functions $\mathbf{h}$ on an open domain $\Omega \subset \mathbb{R}^n$. We conjecture the existence of a transformation that, under adequate additional conditions (such as suitable regularity and non-degeneracy of the kernels), recasts the generalized conformable equation ${}^{h}L_m u = f$ into a corresponding linear Partial Differential Equation of integer order m with classical derivatives, denoted as $L_m^{\text{int}} v = g$, where the solution u of the conformable equation becomes the solution v of the integer-order equation through the appropriate substitution. Although a full proof is beyond the scope of this paper, the second-order construction presented herein suggests an inductive approach: successively applying appropriate coordinate mappings to the factors of higher-order operators. If validated, this conjecture would significantly expand the analytical utility of conformable calculus, offering a powerful methodology to study complex heterogeneity and anomalous phenomena by leveraging the vast analytical tools available for classical integer-order PDEs.

Acknowledgement

The first and second authors would like to express their gratitude to CONAHCYT for the postgraduate scholarship and to Universidad Iberoamericana for the Excellence Scholarship. We would also like to thank DINVP for their support. The authors wish to thank the University of Guadalajara for their financial support through the program PROSNI.

Data availability

The manuscript has no associated data.

Conflict of interest

The authors declare no competing financial interest.

References

[1] Khalil R, Al Horani M, Yousef A, Sababheh M. A new definition of fractional derivative. *Journal of Computational and Applied Mathematics*. 2014; 264: 65-70. Available from: https://doi.org/10.1016/j.cam.2014.01.002.

[2] Anderson DR, Camrud E, Ulness DJ. On the nature of the conformable derivative and its applications to physics. *Journal of Fractional Calculus and Applications*. 2019; 10(2): 92-135.

[3] Luo M, Qiu W, Nikan O, Avazzadeh Z. Second-order accurate, robust and efficient ADI Galerkin technique for the three-dimensional nonlocal heat model arising in viscoelasticity. *Applied Mathematics and Computation*. 2023; 440: 127655. Available from: https://doi.org/10.1016/j.amc.2022.127655.

[4] Nikan O, Rashidinia J, Jafari H. Numerically pricing American and European options using a time fractional Black-Scholes model in financial decision-making. *Alexandria Engineering Journal*. 2025; 112: 235-245. Available from: https://doi.org/10.1016/j.aej.2024.10.083.

[5] Qiu W, Nikan O, Avazzadeh Z. Numerical investigation of generalized tempered-type integrodifferential equations with respect to another function. *Fractional Calculus and Applied Analysis*. 2023; 26(6): 2580-2601. Available from: https://doi.org/10.1007/s13540-023-00198-5.

[6] Yousif MA, Hamasalh FK. Conformable non-polynomial spline method: A robust and accurate numerical technique. *Ain Shams Engineering Journal*. 2024; 15(2): 102415. Available from: https://doi.org/10.1016/j.asej.2023.102415.

[7] Yousif MA, Agarwal RP, Mohammed PO, Lupas AA, Jan R, Chorfi N. Advanced methods for conformable time-fractional differential equations: Logarithmic non-polynomial splines. *Axioms*. 2024; 13(8): 551.

[8] Gateaux R. Sur les fonctionnelles continues et les fonctionnelles analytiques [On continuous functionals and analytic functionals]. *Proceedings of the Paris Academy of Sciences*. 1913; 157: 325-327.

[9] Schreiber A. Multivariate Stirling polynomials of the first and second kind. *Discrete Mathematics*. 2015; 338(12): 2462-2484. Available from: https://doi.org/10.1016/j.disc.2015.06.008.

[10] Todorov PG. New explicit formulas for the *n*-th derivative of composite functions. *Pacific Journal of Mathematics*. 1981; 92(1): 217-236.

[11] Todorov PG. New differential recurrence relations for Bell polynomials and Lie coefficients. *Proceedings of the Bulgarian Academy of Sciences*. 1985; 38(1): 43-45.

[12] Zhao D, Luo M. General conformable fractional derivative and its physical interpretation. *Calcolo*. 2017; 54: 903-917. Available from: https://doi.org/10.1007/s10092-017-0213-8.

[13] Guzmán PM, Napoles-Valdés JE. A note on the oscillatory character of some non conformable generalized Liénard system. *Advanced Mathematical Models & Applications*. 2019; 4(2): 127-133.

[14] Chen W, Zhang XD, Korošak D. Investigation on fractional and fractal derivative relaxation-oscillation models. *International Journal of Nonlinear Sciences and Numerical Simulation*. 2010; 11(1): 3-10. Available from: https://doi.org/10.1515/IJNSNS.2010.11.1.3.

[15] Castillo RE, Valdés JEN, Chaparro H. Omega derivative. *Gulf Journal of Mathematics*. 2024; 16(1): 55-67. Available from: https://doi.org/10.56947/gjom.v16i1.1430.

[16] Gutiérrez-Corona JN, Sánchez-Sánchez OO, Polo-Labarrios MA, Fernandez-Anaya G. Operational temperature optimization in hydrogen turbine blades via time-fractional conformable sensitivity analysis. *Processes*. 2025; 13(5): 1430. Available from: https://doi.org/10.3390/pr13051430.

[17] Sánchez-Sánchez OO, Gutiérrez-Corona JN, Polo-Labarrios MA, Fernandez-Anaya G. Advanced modeling of hydrogen turbines using generalized conformable calculus. *Energies*. 2024; 17(21): 5260. Available from: https://doi.org/10.3390/en17215260.

[18] Liang S, Wu R, Chen L. Laplace transform of fractional order differential equations. *Electronic Journal of Differential Equations*. 2015; 139: 2015.

[19] Barkai E. Fractional Fokker-Planck equation, solution, and application. *Physical Review E*. 2001; 63(4): 046118. Available from: https://doi.org/10.1103/PhysRevE.63.046118.

[20] Myint-U T, Debnath L. *Linear Partial Differential Equations for Scientists and Engineers*. Springer Science & Business Media; 2007.
[21] Risken H, Risken H. *The Fokker-Planck Equation*. Springer; 1996.
[22] Sundnes J. *Solving Ordinary Differential Equations in Python*. Springer; 2024.
[23] Kow PZ, Lin YH, Wang JN. The Calderón problem for the fractional wave equation: uniqueness and optimal stability. *SIAM Journal on Mathematical Analysis*. 2022; 54(3): 3379-3419. Available from: https://doi.org/10.1137/21M1444941.